Biochimica et Biophysica Acta 1807 (2011) 167–188

Contents lists available at ScienceDirect

Biochimica et Biophysica Acta

journal homepage: www.elsevier.com/locate/bbabio

Review

The structural basis of secondary active transport mechanisms

Lucy R. Forrest [a], Reinhard Krämer [c,*], Christine Ziegler [b]

[a] Structural Biology Department, Max Planck Institute for Biophysics, Max-von-Laue Str. 3, 60438 Frankfurt, Germany
[b] Computational Structural Biology Group, Max Planck Institute for Biophysics, Max-von-Laue Str. 3, 60438 Frankfurt, Germany
[c] Institute of Biochemistry, University of Cologne, 50674 Cologne, Germany

ARTICLE INFO

Article history:
Received 16 July 2010
Received in revised form 13 October 2010
Accepted 15 October 2010
Available online 26 October 2010

Keywords:
Secondary active transport
Protein structure
Carrier
Coupling
Modeling
Protein conformation

ABSTRACT

Secondary active transporters couple the free energy of the electrochemical potential of one solute to the transmembrane movement of another. As a basic mechanistic explanation for their transport function the model of alternating access was put forward more than 40 years ago, and has been supported by numerous kinetic, biochemical and biophysical studies. According to this model, the transporter exposes its substrate binding site(s) to one side of the membrane or the other during transport catalysis, requiring a substantial conformational change of the carrier protein. In the light of recent structural data for a number of secondary transport proteins, we analyze the model of alternating access in more detail, and correlate it with specific structural and chemical properties of the transporters, such as their assignment to different functional states in the catalytic cycle of the respective transporter, the definition of substrate binding sites, the type of movement of the central part of the carrier harboring the substrate binding site, as well as the impact of symmetry on fold-specific conformational changes. Besides mediating the transmembrane movement of solutes, the mechanism of secondary carriers inherently involves a mechanistic coupling of substrate flux to the electrochemical potential of co-substrate ions or solutes. Mainly because of limitations in resolution of available transporter structures, this important aspect of secondary transport cannot yet be substantiated by structural data to the same extent as the conformational change aspect. We summarize the concepts of coupling in secondary transport and discuss them in the context of the available evidence for ion binding to specific sites and the impact of the ions on the conformational state of the carrier protein, which together lead to mechanistic models for coupling.

1. Introduction

Secondary transporters are ubiquitously distributed molecular machines found in every cell. They couple the energy of the transmembrane electrochemical potential of one solute to that of another, leading to an uphill flux of the latter and thus to its accumulation in the trans compartment. This process is secondary only in the sense that the source of energy, the electrochemical gradient, must first be generated by ATP-dependent mechanisms, which in turn is known as primary transport. Since the first formulation of the principle events in transport [1], their transformation into concepts of secondary transport mechanisms [2], and the description of the basic principles of the alternating access model for transport [3], the application of numerous biochemical, biophysical and theoretical approaches has enabled the elaboration of the concepts of secondary carrier function. Nevertheless, the basic notion of a transporter being a membrane-bound enzyme that, in contrast to 'normal' enzymes, changes the location, and not the chemical nature of its substrate, is still valid.

In order to gain a deeper understanding of carrier catalysis, however, this basic concept needs to be complemented by detailed knowledge of the biochemical properties and the tertiary structure of transporters. In recent years, the availability of 2D and 3D structures obtained by X-ray and EM crystallography, as well as contributions from computational and theoretical approaches, has greatly enhanced our understanding of the molecular function of these membrane proteins. Despite these advancements, the number of well-resolved 3D structures of membrane-bound transporters is still rather limited in comparison to the numerous high-resolution structures available for soluble enzymes. Moreover, transport is inherently a dynamic process and cannot be completely understood solely on the basis of static pictures, even if they are of high resolution. Consequently, in spite of the growing amount of structural information, we are to a large extent still lacking supplementary information about the dynamic aspects of carrier function.

An important conceptual foundation for the understanding of secondary transport, still valid even considering the most recent developments, is the alternate access model of transport. This model is based on early descriptions of membrane transport function [1,4,5],

* Corresponding author. Institute of Biochemistry, University of Köln, Zülpicher Str. 47, 50674 Köln, Germany. Tel.: +49 221 470 6461; fax: +49 221 470 5091.
E-mail address: r.kraemer@uni-koeln.de (R. Krämer).

0005-2728/$ – see front matter © 2010 Elsevier B.V. All rights reserved.
doi:10.1016/j.bbabio.2010.10.014

and was first formulated in a strict sense by Jardetzky [3]. In this model, the catalytic cycle of a transporter does not involve a significant movement of the substrate binding site relative to the membrane, but rather, upon sequential conformational changes of the carrier protein, a sequential exposure, i.e., alternate accessibility of this site to one side of the membrane or the other. This concept has since been developed and refined based on kinetic and biochemical studies as well as on theoretical considerations, by the description of substrate permeation pathways, gating functions, and specific conformational constraints, leading to detailed descriptions of putative conformational events and related kinetic steps in specific carrier proteins [6–11].

Another essential foundation is the formulation of the energetics of transport. The function of transporters, like that of enzymes, can be described by basic energetic principles, which, in turn, have fundamental mechanistic implications. However, while an elaborate theoretical framework has been developed for enzyme catalysis (e. g. [12]), the application of these principles to transport has received only limited attention [7,9,13–15]. This probably reflects the fact that, in contrast to enzymes, carriers do not change the chemical nature of their substrates and, consequently, a transition state does not appear to make much sense in the context of transport catalysis. Theoretical descriptions and experimental analysis of carrier catalysis, however, have shown that transport proteins in fact work in rather similar ways to enzymes. Just like enzymes, these sophisticated energy converters utilize the energy of substrate binding to reduce the high free energy barrier of the empty carrier protein down to the level of the transition-state complex between the transporter and its substrate, in a way that guarantees suitably high rates of transport [15,16].

Beyond the alternating access model and the fundamental principles of transport energetics, the development of more detailed functional models for a particular transporter requires the availability of a wealth of biochemical data, either from transport kinetics with wild-type and mutant forms of the protein (such as K_d and K_t (K_m of transport) of substrate, V_{max}, substrate specificity, definition of binding order, electrophysiological parameters), or from the application of biochemical and biophysical techniques such as cross-linking, spectroscopy (e.g., fluorescence, FRET, EPR, NMR), covalent modification, accessibility measurements, and many more.

Currently the most stimulating contribution to our understanding of secondary transport is the fast growing amount of structural data on transport proteins. This impact is particularly significant when crystal structures are available for a given transporter in different states, e.g., with and without bound substrate/co-substrate, reflecting various conformational states in the catalytic cycle of transport, or corresponding to different levels of activation.

Building on these structural data, impressive progress in computational techniques is providing an additional source of valuable information, in particular for developing ideas on dynamic and energetic aspects of transporter function. The exploitation of structural data and their use for computational studies will be the major focus of this review.

Indeed, for a number of opportune cases, the combination of results from a multitude of different approaches and sources of information has recently allowed the proposal of elaborate concepts for the function of carrier proteins, or structural elements thereof [17–22]. In this review we will attempt to describe what has been learned by these studies. In spite of the developments of the past few years, we are still far from a true understanding of the microscopic mechanisms of these fascinating molecular machines. Specifically, in our view, three key lines of evidence are still lacking or remain insufficiently described.

First, we do not know enough about the dynamics of carrier proteins as they proceed through the catalytic cycle of transport. This refers both to the question of how many discernable conformational intermediates within the transport cycle we need to consider and what their properties are, and also to the dwell time of these different intermediates within the cycle. We would like to know, for example, which conformational states are transient and which are relatively stable. This latter question is closely connected to an understanding of how particular conformational events in the transport cycle of a carrier correlate with specific energetic states in carrier catalysis, which to date has been derived mainly from theoretical considerations [16].

The second area relates to the diversity of carrier structures. A surprising result of the growing number of available 3D structures of transporters is that many of these proteins – even though they lack significant sequence similarity, and consequently have been assigned to different carrier families – are nevertheless characterized by a similar structural fold. Even more surprising is the observation that what is most probably the core machinery of transport catalysis seems to use a common construction, i.e., an inverted structural symmetry motif within the carrier protein. However, because of the small number of examples, the lack of sufficient resolution of particular structures, or limited information on their dynamic behavior, it is currently not fully clear whether basic mechanistic principles derived for specific transporters, mainly those with the LeuT fold (see below), are in fact valid for all other transporters as well. Although this appears to be merely a theoretical consideration, an answer to this question will have important consequences, for example with respect to understanding the way in which diverse systems have evolved from primordial structural elements in this functional class of proteins.

A third area where information is still scarce relates to coupling, and specifically, the principles that guide the requirement for a specific ion to be co- or counter-transported with the substrate in coupled transport. Aside from considering the conformational events in the catalytic cycle (discussed above), previous kinetic, energetic and biochemical models have also focused on defining the principles of coupling between driving forces and substrate movement. Nevertheless, the question of coupling is, in our opinion, still poorly understood. In particular, the different models currently put forward for specific transporters or carrier families differ significantly in their accounting for the principles of coupling. This has significant consequences for the understanding of important aspects of secondary transport, e.g., for the functional meaning of 'gate elements' during the transport cycle, or for the question of how similar the formally distinct mechanisms of symport and antiport are in molecular terms. In other words: should it be possible to discriminate an antiporter from a symporter on the basis of recognizable structural elements?

In this review we will restrict ourselves to secondary transport. Although there is a significant overlap in basic principles between primary and secondary transport, both with respect to energetic principles and coupling concepts [6,11,13], the differences between these types of transport mechanisms in conceptual, functional, and in particular in structural aspects are significant. For another interesting class of transporters, namely, phosphotransferase systems, not enough structural information is available for a similarly detailed discussion. In addition, for obvious reasons, we will concentrate mainly on those secondary transport systems for which structures at reasonable resolution are available. We will, however, try to discuss as many secondary carriers with known structures as possible, in order to make this a broader review than most previous articles, which have focused on only a couple of examples each. A more generalized view will also help to close the gap between interesting carrier structures and the wealth of biochemical knowledge that is available, at least for some transport systems.

2. A uniform concept for secondary transport mechanism

A common foundation for discussing the mechanism of solute transport has, for more than 40 years, been the model of alternating access [3] (for review see [17,23]). According to this model, the transporter exposes its substrate binding site(s) to one side of the

membrane or the other during transport catalysis. The transition between the two alternate states involves a substantial conformational change of the carrier protein. However, the extent to which the substrate changes its location within the protein during transport catalysis is not necessarily specified by this model, and in principle may differ for different transporters. The kinetic description of the alternating access model has been fleshed out by subsequent biochemical studies [8,10]. It was first demonstrated convincingly on an experimental basis for the mitochondrial ADP/ATP carrier, using side-specific and thus conformation-specific inhibitor compounds [7,24], and was subsequently renamed the single-binding center gated pore (SBCGP) model. This more specific nomenclature emphasizes the fact that the mechanistic concept requires the presence of a central binding site or, more precisely (for functional reasons), a binding center, which is alternately exposed to the two sides of the membrane. The SBCGP model also indicates that the presence of gates is an important feature of carrier catalysis (see below).

We are now in a position to refine the definition of the sequence of conformational and functional states during carrier catalysis that was originally laid out in the alternating access or the SBCGP models, in the light of the recent structural data for transporters. Consequently, to provide a foundation for a later discussion of specific structures and mechanisms, we describe a typical series of conformational states (Fig. 1) in which we differentiate between substrate (or substrates) bound to an open (CSe and CSi) and an occluded form of the carrier (CSce, CSc, and CSci). These different states will be discussed in the context of the energy profile of carrier catalysis described below. It should be pointed out that the configuration of the binding site, and the steric context of the substrate sitting in the carrier protein, may differ in the two alternative conformations, CSec and CSic, since both the substrate and the binding site are typically not symmetric entities, so the profile of the binding site presented to the substrate may be different in the two conformations. In the case that a single substrate is transported during the conversion from CSec to CSic, (i.e., in the absence of a co-substrate) then one of two things can happen: if the return step occurs in the empty form (Ci → Ce) the result is a uniport mechanism; if the return step involves the second, antiport substrate, then the result is an antiport mechanism. In a symport mechanism, the transport cycle is defined by the inclusion of binding and release steps of the co-substrate, which would be similar to those of the substrate. Three of the states indicated in Fig. 1 are potentially not well populated or, at least, may be difficult to observe experimentally; however, we have included them for conceptual reasons. Specifically, the two states CSe and CSi are expected to be transient. In addition, the fully occluded state, CSc, may be a transient intermediate between the two states CSec and CSic, at least for some transporters. Whether experimentally observable or not, these three states, although probably short-lived, are formally necessary intermediates and helpful for describing the energy profile of transport.

As mentioned above, gates may also play an important role in carrier catalysis. It should be noted that the function “gating” was originally introduced in the ion channel field, where it signifies opening or closing of the pore of a channel in response to a particular stimulus (electrical, chemical or mechanical) [25]. Thus, a gate in a channel is a part of the channel pore that obstructs the passage of ions when the channel is closed (or inactivated), and which changes its conformation upon a stimulus to open a passage for the ions through the channel. This designation has since been adopted for carriers, but because of the differences in the function of transporters and channels, it has a rather different meaning in at least two aspects. First, a gate in carrier function is simply a particular (sub)domain of the transporter protein that may regulate the accessibility of the substrate binding site to/from the surroundings. Thus, its function is essentially independent of substrate translocation. However, gating is sometimes also given a second meaning in which it is applied to the core function of carrier proteins, i.e., the massive conformational change of the whole protein as a response to binding or release of the substrate(s). Although this second usage of the expression 'gating' seems similar to its usage for channels, it has a mechanistically different meaning, as will be discussed below in the context of energetic considerations (transfer of binding energy).

The intuitive perception that gating may have both these functions in carrier catalysis, together with the observation that the putative structural correlates of the two functions may be different sizes (see section 3), have led to the somewhat imprecise designation of 'thin' and 'thick' gates. A thin gate in this sense means a part of the protein that can regulate the accessibility of substrates (according to the first meaning of gating described above) from one side of the carrier, e.g., from the 'e' side, if the transporter is in the Ce conformation. Opening or closing of thin gates is not correlated with significant changes of the whole protein. In contrast, a thick gate has sometimes been assigned to a core component of the carrier structure that will undergo substantial conformational change when the transporter switches between the Ce and Ci states (according to the second meaning of gating described above) [18,21]. Thus, in Ce or Ci states of the carrier, the structural unit assigned to the thick gate obstructs the substrate

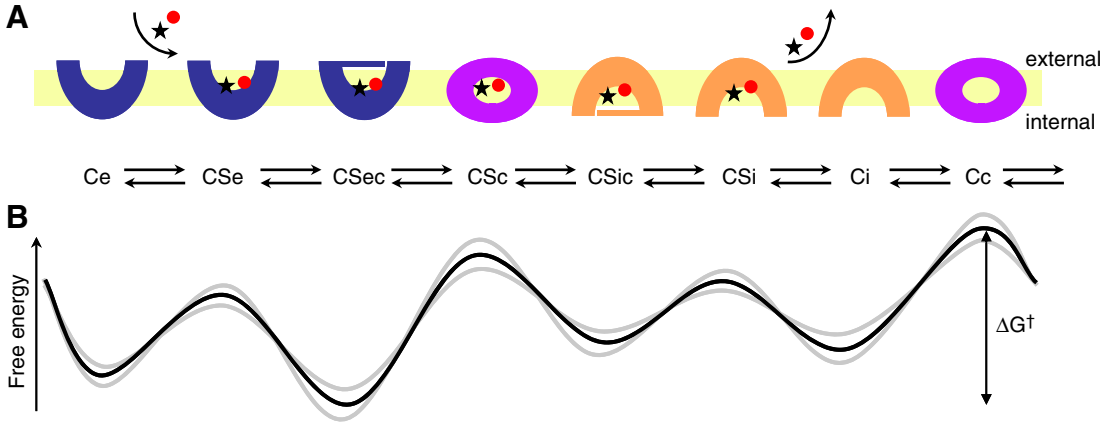

Fig. 1. A series of different conformational states during coupled transport. (A) Substrates (S, star and red circle) bind to an externally open carrier conformation (Ce), forming a transient substrate-bound state CSe, which transforms to an occluded substrate-bound state still facing the external side of the membrane (CSec). Switching from CSec to an inward-facing, occluded substrate-bound state CSic passes through a fully occluded, probably transient, substrate-bound intermediate state, CSc. Substrates are then released from a transient substrate-bound inward-facing open conformation (CSi) and the carrier can switch back from inward open (Ci) to outward open (Ce) state via a fully occluded, intermediate state Cc in the case of symport (see text for details). (B) Theoretical energy profile (black) of different carrier states during catalysis, indicating minima at the gated substrate-bound states, and a putative rate-limiting barrier for the re-conversion of the empty carrier. Note that the barriers and minima will vary for different transporters: alternate situations are represented by additional profiles in gray.

from access to the trans side of the membrane (e.g., in the LeuT fold; see section 3). That is, the thick gate occludes the substrate from the 'i' side if the transporter is in the Ce conformation, and *vice versa*. When compared with the scheme in Fig. 1, the action of a thin gate is represented by the catalytic steps CSe↔CSec and CSi↔CSic, whereas opening and closing of a thick gate represents the CSec↔CSic conversion that passes through the transient CSc state. In general, although thin gates have a uniquely defined function and thus add to the cadre of useful descriptors for transporter function, we prefer to avoid the use of thick gates in our terminology since its definition is redundant with that of the major conformational switch, and since the structural correlates of the thick gates are not trivial to define.

Support for these theoretical concepts, and particularly the conformational switch between the two alternative states, was first shown biochemically for the mitochondrial ADP/ATP carrier, where the entire population of carrier molecules could be switched from an extracellular-facing conformation with the bound inhibitor atractyloside to an intracellular-facing conformation induced by binding of the inhibitor bongkrekate [7]. Importantly, this alternating access of the binding site was only observed in the presence of the substrates ADP or ATP, the binding of which triggered the conformational switch of the carrier protein, thus demonstrating the critical contribution of substrate binding to these conformational events.

By considering the contribution of the substrate-carrier interaction, or, more precisely, of binding energy to carrier catalysis, we begin to view transport in basic energetic terms, and thus arrive at a core understanding of carrier catalysis. As mentioned above, such fundamental energetic concepts originate from treating coupled vectorial processes (transport) as analogous to enzymatic processes. Thus, the energy of substrate binding is used for smoothing the energy profile of the different states during carrier catalysis and to avoid low- or high-energy intermediates along the reaction path, so as to guarantee sufficiently high transport rates [16]. Concomitantly, the concept of transition state was introduced [7,14]. Because the chemical nature of the substrate is not altered during transport, the occurrence of a transition state, as in enzyme mechanisms, is not obvious. However, also in the case of transport processes, a transition state intermediate of the carrier protein structure is required to provide the catalytic energy for the transport reaction (see below). In the current view, the transition state is represented by an occluded state of the carrier-substrate complex (CSc) and includes the associated function of gates, both external and internal. At this point, a gate is simply defined operationally as a barrier between the substrate and the internal or external surroundings, thus preventing kinetic equilibration of bound and free substrate. Its structural meaning will become clear when discussing specific carriers.

It is important to note that, by analogy with enzyme kinetics, the binding site in the two empty conformations of the carrier, Ce and Ci, cannot form optimal interactions with the substrate (it does not 'fit' perfectly) and, consequently, the binding energy cannot be exploited fully in those states. Subsequently, however, binding of the substrate enables a conformational change of the carrier, the intrinsic binding energy is 'stored' in the carrier protein in the form of conformational energy, and thus the energy of the transition state is lowered [16]. In the transition state (occluded state, e.g., CSc) the binding site now achieves an optimal fit to the substrate, as in enzyme mechanisms. In contrast to enzyme catalysis, however, the configuration of the substrate remains unchanged, or, in other words, the conformational work is exclusively confined to the carrier protein. By this mechanism, the binding energy is utilized to facilitate specific conformational changes of the transporter during its cycle from the external, via the occluded, to the internal conformation, or *vice versa*. The energy difference related to the sequence of conformational events in which the transport protein changes, upon substrate binding, between states of limited interaction with the substrate and the transition state characterized by an intimate substrate-protein interaction, represents the catalytic energy for transport. It is paid for by the intrinsic binding energy of substrate-carrier interaction. This concept has been introduced and described in terms of the so-called 'induced transition fit' mechanism [14].

Some important consequences of the induced transition fit concept should be mentioned here. The substrate has only a poor affinity to the carrier in the ground state(s), Ce and Ci, but it should bind strongly to the carrier in the transition state. Consequently, good substrates are discriminated from poor ones in general not by their difference in binding to the ground states (empty carrier) but by their interaction in the transition state (occluded state). Thus, transporter specificity for different substrates is reflected in differences in rates (V_{max}) and not in half-saturation constants (K_m) [26]. Interestingly, this also means that good competitive inhibitors of transport may differ structurally from the corresponding substrate, since they can inhibit by providing optimal interactions with the ground state of the carrier that lead to an energetic trap (i.e., a low-energy state).

It was our intention in this section to lay out a conceptual framework within which we can make sense of the wealth of structural data that will be discussed below. We will first describe current views of the structural basis of transport function, with a focus on the conformational changes involved in the catalytic cycle of carriers. Second, we will attempt to use knowledge of carrier structure and conformational dynamics to better understand the role of functional coupling between electrochemical potentials and concentration gradients of substrates and co-substrates. It is the goal of this review to address questions on possible structural correlates of the principles of solute transport as well as coupling and thus to bridge the gap between concepts and their molecular understanding.

3. Towards a molecular understanding of secondary transport through structure

Lack of atomic structural data has, for many years, created a frustrating divide between the concepts of secondary transport and a molecular understanding of its mechanisms. The recent increase in the number of available transporter structures (Table 1), however, has raised hope in our ability to bridge this gap. Reassuringly, most of the structures reported to date appear to be perfectly consistent with the alternating access model, and confirm the existence of the conformational states originally suggested on the basis of the alternating access or SBCGP models [17–20,27–34]. They are apparently also consistent with the proposal that substrate binding facilitates the conformational changes in the carrier. In fact, evidence for both types of conformational event, i.e., the opening or closing of thin gates, and the concerted conformational switch between Ce and Ci states, is found in carrier structures corresponding to the endpoints of those conformational changes [19,27].

This agreement with the alternating access model seems to be valid for transporters from a wide range of structural families. Sequence data has revealed that secondary transporters are encoded for by a very large number of unrelated gene families, which themselves exhibit broad sequence variability [35]. Therefore, it was not unexpected when transporters from different sequence families were revealed to have different structural folds (Table 1). Nevertheless, in several cases a common underlying fold has been observed for gene families previously believed to be unrelated. A notable example is the so-called LeuT fold of inverted-topology repeats of five transmembrane helices, which has been found for seven different transporters to date, from five different sequence families [18–20]. As of 2010, these contribute to the X-ray crystal structures of 17 different secondary transporter proteins, which can be classified into eight different structural folds (Table 1).

In general, a molecular mechanism of transport should be based on structural data of, at least, the two alternative open conformations, Ce and Ci. Whether it is necessary to have structural data of both

Table 1
Representative structures of secondary coupled transporters.

	Transporter/family	Coupled transport	Fold	Conformational state (in complex with substrate) [in complex with inhibitor]	Res. (Å)	PDB entry [citation]
1	AcrB/RND	H^+/drug antiport	RND	—	3.5	1IWG [166]
					2.9	2GIF [116]
2	EcClC/CLC	H^+/Cl^- antiport	CLC	—	3.5	1KPK [120]
					3.0	1KPL [120]
3	GlpT/MFS	Glycerol-3-phosphate/phosphate antiport	MFS	Ci	3.3	1PW4 [49]
4	LacY/MFS	H^+/sugar symport	MFS	CSi (thiodigalactoside)	3.6	1PV7 [51]
				Ci	3.5	1PV6 [51]
				Ci	3.6	2V8N [52]
				Ci	3.3	2CFP [53]
				Ci	2.95	2CFQ [53]
5	AAC1/MCF	ADP/ATP antiport	MCF	Ce [carboxy-atractyloside]	2.2	1OKC [36]
				Ce	2.8	2CE3 [39]
6	NhaA/NHA	Na^+/H^+ antiport	NHA	Ci	3.45	1ZCD [102]
7	EmrE/SMR	H^+/drug antiport	SMR	— (tetraphenylphosphonium)	3.8	3B5D [105]
				—	4.5	3B61 [105]
				— (tetraphenylphosphonium)	4.4	3B62 [105]
8	EmrD/MFS	H^+/drug antiport	MFS	Cc	3.5	2GFP [50]
9	Glt_{Ph}/EAAT	Na^+/aspartate symport	Glt_{Ph}	Ce	3.8	IXFH [75]
				Ce [(3S)-3-(benzyloxy)-L-aspartic acid]	3.2	2NWW [76]
				CSec (aspartic acid, Na)	3.29	2NWX [76]
				CSec (aspartic acid)	2.96	2NWL [76]
				CSi (aspartic acid and sodium)	3.51	3KBC [77]
10	FucP/MFS	H^+/sugar symport	MFS	Ce [*n*-nonyl-β-D-glucopyranoside]	3.14	3O7Q [54]
				Ce [*n*-nonyl-β-D-glucopyranoside]	3.2	3O7P [54]
11	LeuT/NSS	Na^+/leucine symport	LeuT	CSec (L-leucine, Na)	1.65	2A65 [82]
				CSe (L-tryptophan, Na)	2.0	3F3A [93]
				CSec (L-alanine, Na)*	1.9	3 F48 [93]
				CSec (L-alanine, Na) [clomipramine]†	1.85	2QEI [94]
				CSec (L-leucine, Na) [desipramine]	2.9	2QJU [96]
				CSec (L-leucine, Na) [R-fluoxetine]**	2.35	3GWV [97]
				S2 (leucine, Na and octylglycoside)	2.8	3GJC [95]
12	vSGLT/SSS	Na^+/glucose symport	LeuT	CSic (β-D-galactose, Na)	2.7	3DH4 [83]
13	Mhp1/NCS1	Na^+/hydantoin symport	LeuT	Ce (sodium)	2.85	2JLN [84]
				CSec ((5S)-5-benzylimidazolidine-2,4-dione, Na)	4.0	2JLO [84]
				Ci	3.8	2X79 [21]
14	BetP/BCCT	Betaine-glycine/Na^+ symport	LeuT	CSic	3.35	2WIT [85]
15	AdiC/APC	Arginine/agmatine antiport	LeuT	Ce	3.2	3HQK [89]
				Ce	3.61	3LRB [90]
				Ce	4.0	3LRC [92]
				CSec	3.0	3LIL [92]
16	ApcT/APC	H^+/amino acid symport	LeuT	Cic	2.32	3GIA [88]
17	CaiT/BCCT	L-carnitine/γ-butyrobetaine antiport	LeuT	CSi	3.15	3HFX [86]
				Ci	2.3	2WSW [87]
				CSi	3.4	2WSX [87]

Structures from the LeuT fold are marked in red.
RND: resistence nodulation division family.
CLC: chloride channel family.
MFS: major facilitator family.
MCF: mitochondrial carrier family.
NHA: sodium hydrogen antiporter family.
SMR: small multidrug resistance exporter family.
EAAT: Excitatory amino acid transporter family.
NSS: neurotransmitter solute symporter family.
SSS: sodium solute symporter family.
NCS-1: nucleobase cation symport 1 family.
BCCT: betaine-choline-carnitine transporter family.
APC: amino acid polyamine organocation transporter family.
* 3F3C (phenylalanine); 3F3D (methionine); 3F3E (leucine); 3F4J (glycine) [93].
† 2Q6H [clomipramine]; 2Q73 [imipramine]; 2QB4 [desipramine] [94].
** 3GWU [sertraline]; 3GWW [S-fluoxetine] [97].

of these conformations in complex with substrates (CSe and CSi), in order to have a conclusive description of the conformational changes may depend on the nature of the substrate, the transporter, or the transporter mechanism in question. Currently, structures representing both Ci and Ce conformations are only available for a subset of the known transporter folds (Table 1). Even when structures are available, the limited resolution of those structures in some cases still precludes a reliable description of the conformational changes between the two states. Thus, so far, it has only been possible to develop convincing molecular descriptions of the structural states involved in transport for four different folds, namely the mitochondrial nucleotide carrier family (MCF) fold, the major facilitator superfamily (MFS) fold, the excitatory amino acid transporter family (EAAT) fold, and the LeuT fold.

3.1. Mitochondrial carrier fold: Salt bridge networks and the SBCGP model

The ADP/ATP antiporter was the first secondary transporter to be described by the single-binding center gated pore (SBCGP) model, in which a central binding site is alternatively exposed to the two sides

of the membrane. From biochemical studies with conformation-specific inhibitor ligands, two distinct conformational states were defined: in the Ce state the carrier accepts its substrate from the cytoplasm, and in the Ci state the substrate can access the carrier from the mitochondrial matrix [7,24]. The X-ray crystal structure of the bovine mitochondrial ADP/ATP carrier (BtAAC1) solved to 2.2 Å resolution (PDB entry 1OKC [36]) reveals a monomeric bundle of six α-helices exhibiting a three-fold pseudo-symmetry (Fig. 2A–C). Assuming the monomeric form of this protein is the physiologically relevant one (see below), this large cavity is a reflection of probably the largest substrate-to-protein size ratio of all the known carriers, with the substrate being considerable in size with respect to the protein structure.

The functional oligomerization state of the ADP/ATP carrier has for many years been a matter of intense debate [37,38]. Thus, the presence of artificial protein–protein interactions in the crystal packing of the monomeric X-ray structure raised questions about the physiological relevance of this conformation [39]. However, corroboration was later obtained from a structure in which monomer-monomer contacts in the crystal are mediated by endogenous cardiolipin molecules (PDB entry 2C3E [39]).

Three homologous repeats, each containing the signature motif PX[DE]XX[RK] had previously been identified in the primary structure of the mitochondrial carriers (Fig. 2A and B) [40] and the structure revealed the functional relevance of these motifs [41]. First, the proline residues of the motif allow the C-terminal parts of the transmembrane (TM) helices to kink near the base of the cavity, and second the charged residues of the signature motif connect these helices together via a salt bridge network (Fig. 2C) [36,42].

The structure of BtAAC1 also provided detailed information on how the inhibitor CATR, which is known to bind to the carrier in the Ce state only, may prevent ADP binding. CATR is bound in a large aqueous cavity, which is wide open (with a 20 Å diameter) to the cytoplasm, and closed by a ~10-Å-thick barrier to the mitochondrial matrix formed by the salt bridge network mentioned above. Thus, this structure likely corresponds to the Ce state of the transport cycle [36]. However, although molecular dynamics simulations of spontaneous ADP binding [43], and analysis of the structural features of CATR [44], both suggest that ADP binds at the same binding site as CATR, this has not yet been confirmed by structural analysis, and therefore we do not yet have conclusive support for the SBCGP model. The CATR-BtAAC1 structure may also provide an example of an inhibitor trapping the carrier in a low-energy state, thus preventing binding of the substrate, as discussed in section 2. However, in the absence of structural data for the CSe state for comparison, it is not possible to say conclusively that the CATR interactions for Ce favor one state more than those that would be provided by ADP.

In the absence of a structure of the Ci state of BtAAC1, the structural changes required for the translocation of the substrate also remain speculative [42,44]. However, a plausible mechanism has been proposed based on symmetry arguments. Specifically, it was assumed that triplets of highly conserved, symmetry-related residues are likely to be important for a common mechanism of transport, unlike the residues involved in substrate binding, which will be asymmetrically distributed (reflecting the asymmetry of the substrates) [41]. This analysis revealed, in addition to the known signature motif on the matrix side, a second symmetrically distributed and conserved cluster of charged residues that flank the putative substrate binding site on the cytoplasmic side (Fig. 2C). The charged residues of the second motif were proposed to form a salt bridge network when the transporter is in the Ci state (matrix state), playing a symmetrically equivalent role to that of the signature motif observed in the Ce structure. Thus, formation and disruption of these two networks may allow the major conformational switch during the transport cycle [41]. Kinetic studies have demonstrated that many mitochondrial carriers function in a strict exchange mode and therefore only one substrate may be bound at a time [45,46]. Binding of phosphate anions with three or four negative charges, as in ADP and ATP, respectively, can be expected to provide sufficient energy via electrostatic interactions to overcome the initial activation energy barrier posed by the salt bridge networks [43], while there is only a low probability of disrupting the networks spontaneously [47] and therefore the transition from outward to inward should only occur when substrate is bound. However, because the binding site is not known it remains unclear specifically how binding of the substrates triggers the conformational changes required for ADP/ATP antiport.

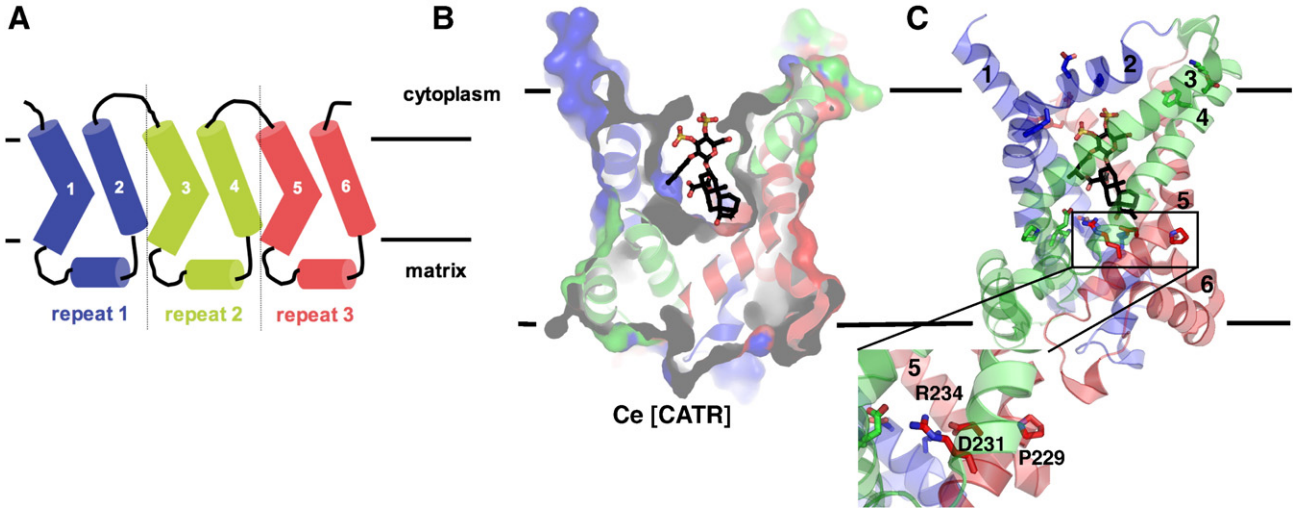

Fig. 2. Overall fold, conformation and inhibitor binding in the bovine mitochondrial ADP/ATP carrier (BtAAC1). (A) BtAAC1 exhibits a topology of six α-helices formed by three sequence- and structure-related repeats. (B) Cross-section through the surface representation of the X-ray structure of the bovine mitochondrial ADP/ATP carrier (BtAAC1) in complex with the inhibitor carboxy-atractyloside (CATR) solved to 2.2-Å resolution (PDB entry 1OKC). This structure represents a cytoplasmic open conformation (Ce). The inhibitor (displayed in stick representation with carbon atoms in black, oxygen in red and sulphur in yellow) is bound in a large cavity. The boundaries of the membrane are indicated with black lines. (C) The two helices of each repeat, colored according to (A), contribute to a six-helix bundle that is arranged as in an iris diaphragm. Each repeat contains the signature motif PX[DE]XX[RK] in the odd-numbered helix (TM1, 3, 5), which is shown for repeat 3 in TM5 (Pro229, Asp231, and Arg234) in the inset. The interaction of the charged residues via salt bridges effectively occludes the carrier from the matrix side. An additional consensus motif [FY][DE]XX[RK] is observed on the cytoplasmic side in the even-numbered helices (TM2, 4, 6), and is suggested to be responsible for occluding the carrier from the cytoplasmic side in a similar mechanism.

In summary, the structural data for BtAAC1 provides direct confirmation of the existence of a Ce conformation in alternating access. Furthermore, the three-fold symmetry of the interactions in the structure has inspired the formulation of a specific mechanism for the conformational switch to the alternative state.

3.2. The MFS fold: The rocker-switch mechanism

Several X-ray crystal structures have been reported for members of the MFS family, which represents the largest evolutionarily related superfamily of secondary transporters [48]. Specifically, structures are available for four *E. coli* carriers: the glycerol-3-phosphate/inorganic phosphate antiporter GlpT (PDB entry 1PW4, [49]), the drug/H^+ antiporter EmrD (PDB entry 2GFP [50]) and the lactose/H^+ symporter LacY [51–53], and very recently for the fucose/H^+ cotransporter FucP (PDB entries 3O7P and 3O7Q [54]). For LacY, which has probably been more intensively studied than any other secondary carrier, five structures of wild-type and mutant proteins have been solved to date, under different conditions (PDB entries 1PV6 and 1PV7 [51], 2V8N [52], 2CFP, and 2CFQ [53]). In all these structures, the N- and C-terminal halves of the protein each form a structural repeat consisting of a six-helix bundle (Fig. 3A and B). These two terminal domains are related by a pseudo-twofold symmetry axis running through the center of the transporter, perpendicular to the membrane, and are in close contact at the periplasmic side of the membrane.

While GlpT has only been crystallized in an apo state to date, LacY has also been crystallized with a single molecule of a lactose homolog (ß-D-galactopyranosyl-1-thio-ß-D-galactopyranoside, TDG) bound. TDG was found in the cavity near the approximate center of the protein, which was therefore proposed to be the substrate binding site [51]. This site is found to be a similar distance from either side of the membrane and is close to the approximate molecular two-fold axis of the structure. Because in both GlpT and LacY structures the putative substrate translocation pathway is closed from the periplasmic side and access of substrate from the periplasm is prevented, while the pathway is clearly accessible to solutes from the cytoplasmic side, these structures were assigned as either Ci or CSi conformations (Fig. 3B). In the available structure of EmrD [50], by contrast, the center of the carrier is closed to both sides of the membrane, reminiscent of an occluded state (Fig. 3B). Finally, the recent FucP structure appears to represent an outward-facing conformation, i.e., a Ce state [54]. The structure of the CSi conformation of LacY (PDB entry 1PV7) was originally made possible by the introduction of a point mutation (C154G) that resulted in a thermostable mutant that binds substrate with high affinity but is trapped in one conformation [55,56]. The substrate-free Ci state of LacY was later captured in

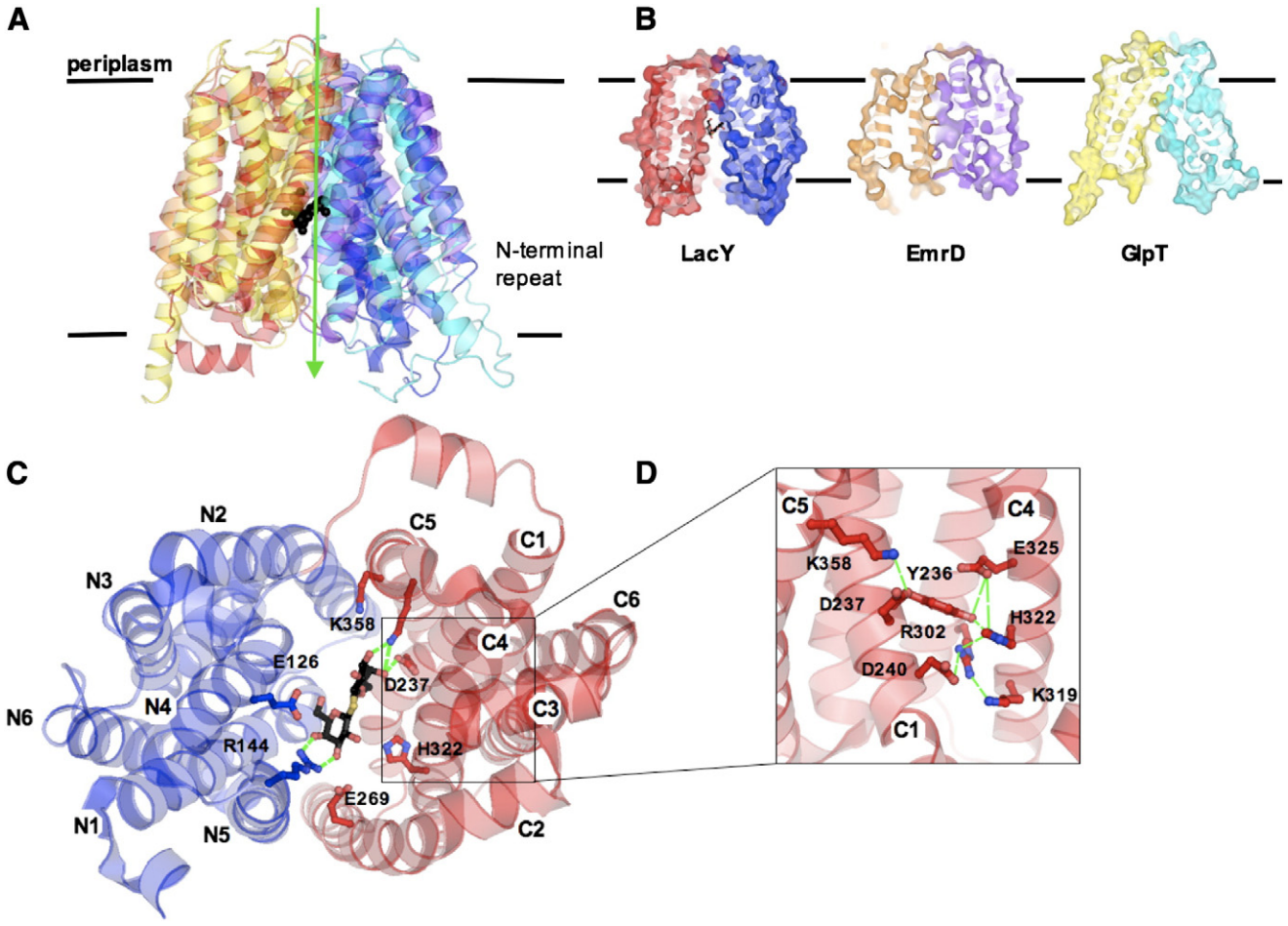

Fig. 3. Overall fold, conformations and substrate binding in the MFS family. (A) Overlay of structures of LacY (PDB entry 1PV7), GlpT (1P4W) and EmrD (2GFP) in ribbon representation viewed along the plane of the membrane. The six TM helices of the N-terminal domain are colored in blue (LacY), cyan (GlpT) and purple (EmrD). The six TM helices of the C-terminal domain are colored in red (LacY), yellow (GlpT) and orange (EmrD). The LacY substrate TDG is represented by black spheres. (B) Cross-section through the surface representation of the X-ray structures of LacY, EmrD and GlpT. TDG is displayed in stick representation and is accessible from the cytoplasm in LacY. The color scheme is the same as in (A). (C) Residues in LacY involved in TDG binding, viewed along the membrane normal, from the cytoplasmic side. The six TM helices are labeled. The N- and C-terminal domains of the transporter are colored blue and red, respectively. (D) Side view from the cytoplasmic cavity toward the proton translocation site composed of charged residues located in TM7 (C1), 10 (C4) and 11 (C5) in the C-terminal repeat colored in red. The network of hydrogen bonds and salt bridges is shown as dashed green lines.

structures of wild-type LacY at basic pH (8.5), as well as of the mutant C154G at neutral (6.5) and acidic (4.5) pH (PDB entries 2V8N, 2CFQ and 2CFP, respectively [52,53]).

Several important conclusions could be drawn from comparison of these structures. First, the fact that LacY and GlpT share a common structural fold demonstrates that both symport and antiport can be achieved with the same protein architecture (Fig. 3A) [17,28,33]. Second, the Ci conformation might represent a low free energy state for MFS transporters, since that state has so far crystallized in substrate-bound or apo form to high resolution [17], while the Ce conformation has been reported so far only in the presence of a putative inhibitor *n*-nonyl-β-D-glucopyranoside (β-NG) [54]. This would be consistent with the fact that the presence of substrate increases the population of the Ce state (see below). Third, the strong similarity (at 2.95–3.6 Å resolution) of the mutant LacY structures in the substrate-bound CSi and the substrate-free Ci states, limits the possible conformational changes upon substrate binding to form the CSi state (but not the full transition to CSe) to movements of <3.6 Å. The fourth finding relates to coordination of the substrate [51]. In the CSi conformation of LacY, TDG hydrogen bonds with the side chains of ionizable residues (Fig. 3C). Furthermore, the two galactopyranosyl rings of TDG bind to some extent to both the N- and C-terminal halves of the protein and therefore provide a means to communicate conformational changes between the domains. Finally, numerous atoms of the galactopyranosyl ring in the observed CSi conformation do not interact directly with the protein and, as shown by molecular dynamics simulations, are therefore instead solvated by water [57–59]. Therefore, we suggest that the coordination of TDG observed in the LacY CSi state represents an 'imperfect fit' according to the 'induced transition fit' mechanism. It would clearly be of interest to observe the interactions of the ligand with LacY in an occluded state (preceding CSic), as the binding site there should, by this logic, interact optimally with the substrate.

Insights into the structure of the occluded conformation of MFS transporters have been obtained from a 6.5-Å 3D electron microscopy map of the oxalate/formate antiporter OxlT from *Oxalobacter formigenes* [60] and a 3.5-Å X-ray structure of the drug/H^+ antiporter EmrD from *E. coli* [50]. Unlike the trapezoid shape (as observed from the plane of the membrane) of the Ci structures of GlpT and LacY, the structures of OxlT and EmrD are more rectangular in shape, and thus more symmetric (Fig. 3B) [17]. It is important to note that substrate is not visible in either of the occluded structures. Nevertheless, since antiporters should never adopt an empty occluded state (Cc), transient or otherwise, the absence of substrate in these structures is most likely a consequence of insufficient resolution [17].

As mentioned above, the known structures of MFS transporters correspond to four distinct conformational states, CSi, Ci, C(S)c and, very recently, Ce. The conformational changes implied by these structures – albeit from different proteins – are supported by a large body of biochemical and spectroscopic data indicating that LacY undergoes conformational changes upon sugar binding that lead to closing of the observed cytoplasmic cavity and opening of a large hydrophilic periplasmic cavity in order to create a Ce state [61–63]. Specifically, site-directed alkylation [55,61,64–66], single-molecule Förster resonance energy transfer [67,68], double electron-electron resonance [69], tryptophan fluorescence [70], ligand-induced fluorescence measurements [71,72], site-directed thiol cross-linking and analysis of cross-linked distances in the Ci state structure [62,63,73], all provide independent evidence that sugar and proton translocation by LacY involves such an outward-facing conformation.

These structural and biochemical data have together made it possible to describe a hypothetical translocation mechanism for MFS transporters, which was the first structure-based molecular mechanism of secondary transport to be proposed, and which confirms the alternating access model and the SBCGP model to a large extent [28]. This so-called "rocker-switch" mechanism postulates that the symmetry-related N- and C-terminal halves of the transporter rock back and forth against each other along the two-fold axis that runs along the domain interface (Fig. 3A). Thus, from the observed Ci conformation in which the periplasmic sides of the two domains close the pathway, pivoting (or rocking) of the domains around the approximate substrate binding site would result in the Ce conformation in which the domains become close together at the cytoplasmic side instead [54]. The global conformational changes in this rocker-switch mechanism may be caused by the formation and breaking of inter- and intra-domain salt bridges [72]. For example, it has been proposed for LacY that salt bridge interactions that characterize the Ci state might weaken due to high-affinity substrate binding (e.g., between Arg144 and Glu126, Fig. 3C) [69]. Such a role for the substrate, as well as explaining how the energy of binding may be translated into the conformational change, is also consistent with the 'induced transition fit' mechanism. In addition, the swiveling motion of each domain relative to the other would result in different configurations of the binding site residues in Ce and Ci.

Although the conformational changes predicted by the rocker-switch model are in perfect agreement with the alternating access model, the former does not reflect the presence of the occluded state, which according to the EmrD [50] and OxlT [60] structures, suggest a clam-shell arrangement around the substrate. A more symmetrical intermediate state is also supported by double electron-electron resonance measurements [69], and by molecular dynamics simulations of MFS transporters [57,59,74]. Thus, the domains would not move as rigid bodies, but instead close around the substrate before opening up again on the other side.

In summary, the structures of the MFS fold confirm the presence of a central binding site – as hypothesized in the SBCGP model – in which the substrate is fully accessible in the CSi state. Moreover, the observed CSi state provides an example of a low-energy conformational state in which the substrate is 'imperfectly' coordinated. However, because of the lack of structural information about both the Ce state of LacY and the site of proton binding [71], the precise molecular mechanism by which substrate binding relates to the global conformational change between the CSi and CSe states, has yet to be demonstrated structurally.

3.3. Conformational changes in transporters of the excitatory amino acid transporter (Glt_{Ph}) fold

The sodium/aspartate symporter from *Pyrococcus horikoshii* (Glt_{Ph}), an archaeal homologue of the EAATs, was one of the first sodium-coupled transporters for which a 3D structure was determined (PDB entry 1XFH [75]). The X-ray crystallographic data revealed a homotrimeric structure that forms a deep solvent-filled bowl open to the extracellular solution. In each Glt_{Ph} protomer the first six transmembrane helices (Fig. 4A and B, blue and cyan helices) form a distorted cylinder, which in turn encloses a compact core domain containing two re-entrant helical hairpins, called HP1 and HP2 (Fig. 4A and B, yellow and red helices).

Crystal structures of Glt_{Ph} have been reported in three different conformations (Fig. 4A and D). In the first (PDB entry 2NWX [76]), an L-aspartate molecule and two thallium ions (i.e., as sodium replacements) are bound to each protomer near the tips of the two hairpins HP1 (Fig. 4A–D, yellow) and HP2 (Fig. 4A–D, red). On the extracellular side of the membrane, the substrate is occluded from the aqueous environment only by HP2, while more than 15 Å of protein separates the substrate from the cytoplasm, all of which suggests an occluded, CSec state of the transporter. In a second crystal structure of Glt_{Ph} in complex with a non-transportable substrate analogue L-threo-β-benzyloxyaspartate (TBOA; PDB entry 2NWW [76]), the HP2 hairpin (Fig. 4D, red) assumes a more "open" conformation, suggesting that this structure mimics the Ce state in which the substrate binding site would be accessible from the extracellular solution. In contrast to the

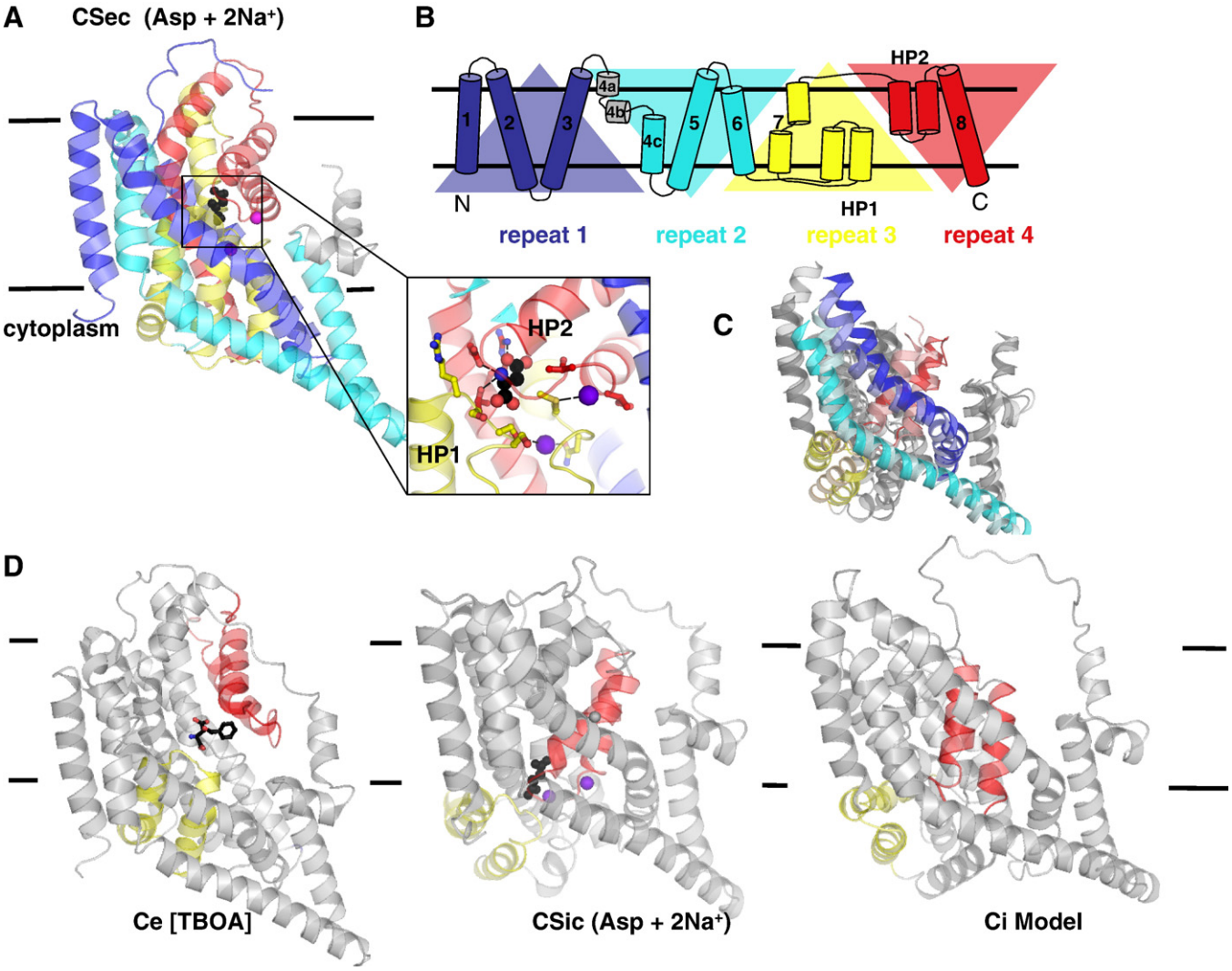

Fig. 4. Overall fold, conformations and substrate binding in Glt_{Ph}. (A) View along the plane of the membrane of the X-ray structure of the Glt_{Ph} protomer (PDB entry 2NWX) in complex with two thallium ions (replacing sodium; purple spheres) and an aspartate molecule displayed as black spheres. The helices of each repeat are colored according to the topology. Inset: The substrate binding sites for aspartate (black spheres with oxygen atoms in red and nitrogen in blue) and sodium (purple spheres) are located between the two helical hairpins HP1 (yellow) and HP2 (red). (B) The topology of Glt_{Ph} is characterized by the presence of repeated structural units, shown in different colors. (C) Overlay of the X-ray structure of the CSic conformation (3KBC, light grey with TM2 in light blue and TM5 in pale cyan) with a model of the same conformation built using the inverted-topology repeats in the X-ray structure (dark grey with TM2 in blue and TM5 in cyan). Model and structure can be superimposed with a r.m.s.d. of 5.4 Å (excluding the loop between TMs 3 and 4), a small amount relative to the 15–20 Å movements of the transport domain, which demonstrates that conformational changes of the two symmetry-related states involve the inverted-topology repeats. (D) Side view of structures of Glt_{Ph}: in complex with the inhibitor TBOA in stick representation (2NWW), thought to resemble the Ce state; and in a CSic conformation (3KBC) in complex with two sodium ions (purple spheres) and an aspartate molecule (black spheres). The model of an inward-facing (Ci) state, built using the equivalent Ce structure (2NWW) as a template, is shown on the right. HP1 and HP2 are colored in yellow and red, respectively.

situation for BtAAC1 (see above), then, we can conclude that TBOA inhibition occurs by trapping Glt_{Ph} in the empty Ce state, which differs from e.g., the CSec state that interacts more favorably with the substrate, consistent with the proposal from enzyme kinetics (section 2). Finally, in the last year, the structure of the CSic state – that is, after the major conformational switch – was solved by crystallography of a cross-linked double-cysteine Glt_{Ph} mutant (55C/364C-Hg, PDB entry 3KBC [77]).

Unexpectedly, the conversion between the CSic and CSec states of a Glt_{Ph} protomer requires a piston-like movement of the entire substrate binding domain by >15 Å across the membrane (Fig. 4D). Remarkably, this large conformational change was correctly predicted by structural modeling based on symmetry arguments: that is, swapping the conformations of pairs of symmetric structural elements that were identified in the CSe structure (Fig. 4A and B; see below) resulted in a model of the CSi conformation that captures the major features of the cross-linked Glt_{Ph} mutant (Fig. 4C) [78] (Protein Model Database (PMDB) code PM0075966; see http://mi.caspur.it/PMDB). This approach was also used to construct a structural model of the Ci state of Glt_{Ph}, in which HP1 is open and exposes the substrate binding site to the cytoplasm (Fig. 4D, PMDB code PM0075968), thus completing the set of structures in the transport cycle [78]. The success of this approach for modeling alternate conformations has fascinating implications for the role of symmetry in secondary transport, as will be discussed below.

There is a novel aspect to the mechanism of Glt_{Ph} transport, compared to the rocker-switch mechanism discussed for the MFS transporters, and that is the proposed role of conformational changes in small sub-domains of the Glt_{Ph} structure (the helical hairpins) to allow, or prevent, access to the substrate binding site in response to a specific event during transport. Thus, the hairpins are said to function as thin gates although, from a structural point of view the definition of such gates is still rather imprecise. Note that, if the same concept of thin gates were to be applied to MFS transporter function, it might

involve changes only in side chain configurations [62], whereas in Glt_{Ph} the backbone of the helical hairpin can move. Thus, the size of a gate (i.e., whether a channel is prevented from forming by, e.g., side chain or backbone elements) is likely to vary for different transporters and may be reflected in the binding kinetics. The assignment of HP2 as a thin extracellular gate was inferred from comparison of the CSec and Ce structures [75] (Fig. 4A and D), and is supported by the markedly dynamic nature of HP2 in simulations of substrate-free Glt_{Ph} [79,80], as well as fluorescence changes in reporter groups covalently linked to HP2 [81]. The most recent models and structural data indicate that HP1 forms the intracellular gate in a symmetry-related way [77,78]. Interestingly, a consequence of the Glt_{Ph} mechanism is that the interactions with helices of the N-terminal cylinder keep one of the two gates locked shut at any given time, similar to the doors in an air lock. Moreover, during the shuttling of the transport domain there are likely to be many intermediate conformations in which both hairpins are locked shut by those same interactions, implying that the Glt_{Ph} alternating access mechanism is inherently efficient at preventing leakage.

Molecular dynamics simulations indicate that binding of substrate and sodium ions, which are thought to trigger the major conformational change from CSec to CSic, may also be required for the closure of the corresponding thin gates [80], e.g., the transition from Ce to CSec by closure of HP2 (Fig. 4A and D). While the 'induced transition fit' mechanism suggests that the intrinsic binding energy of substrate-carrier interaction drives the CSec → CSic conformational change, we propose that for Glt_{Ph} this energy is required to keep the extracellular gate closed (Ce → CSec) and thus to form the substrate binding site (see section 4). Once the hairpin gate is closed, there should be no additional energy required. Thus, the CSec → CSic transition in which the "closed" transport domain moves against the fixed parts of the structure, will presumably occur stochastically, as a result of thermal energy alone, although this does not necessarily mean that the transition is rapid. An equivalent transition has been suggested to occur for the apo transporter (Glt_{Ph}) in order to complete the transport cycle [77].

In the Glt_{Ph} fold, gating and substrate translocation are inherently linked, due to the fact that the gates (HP1 and HP2) also contribute to the substrate binding site (Fig. 4A, inset). Moreover, the whole binding domain including both gates, acts as a carrier module that shuttles the substrates towards the cytoplasm during the CSec → CSic transition, resulting in a significant change in the location of the substrate during translocation (Fig. 4D). Thus, transport by Glt_{Ph} does not obey the central binding site requirement proposed in the SBCGP model.

In summary, although structural data for the Glt_{Ph} fold confirmed aspects of the concept of gating during the alternating access mechanism (i.e., in the Ce → CSec transition), other aspects of the transport mechanism described in this section are most likely specific to the Glt_{Ph} fold.

3.4. Conformational changes in LeuT fold transporters

For a long time, the rocker-switch and Glt_{Ph}-type gating mechanisms were presented as two opposing models for the function of secondary transporters. This situation changed with the increase in structural data for transporters with the LeuT fold, starting in 2005 [82]. This fold was first observed for LeuT from *Aquifex aeolicus*, a bacterial homologue of the neurotransmitter sodium symporter (NSS) family, and was subsequently found in six other proteins (Table 1): the Na^+/galactose symporter vSGLT [83] from *Vibrio parahaemolyticus* of the solute/sodium symporter (SSS) family, the benzyl-hydantoin transporter Mhp1 [84] from *Microbacterium liquefaciens* of the nucleobase/cation symporter (NCS1) family, the Na^+/glycine betaine symporter BetP [85] from *Corynebacterium glutamicum* and the L-carnitine/γ-butyrobetaine antiporter CaiT [86,87] from *E. coli* or *Proteus mirabilis*, both members of the betaine-choline-carnitine transporter (BCCT) family, the H^+-coupled amino acid transporter ApcT [88] from *Methanocaldococcus jannaschii* as well as in the arginine/agmatine antiporter AdiC [89,90] from *E. coli*, both of which are members of the *amino acid, polyamine, and organocation* (APC) transporter family.

Although differing in total number of TM helices, all the LeuT fold transporters share a repeated structural motif of five TM helices. The first five TM helices are related to the second five by a two-fold pseudo-symmetry axis, running parallel to the membrane plane. In many cases the first helix of each of these repeat units contains unwound helical regions that are responsible for forming substrate interactions [18]. Such unfolded stretches of protein expose main-chain hydrogen-bonding partners, creating a polar environment suitable for coordination of substrate and ions [91].

The first two helices of each repeat in LeuT come together to form a four-helix bundle that is surrounded by an outer scaffold of helices (Fig. 5A). Depending on the specific structure, this helix bundle either contains within it (e.g., for BetP), or lines one side of (e.g., for LeuT), the central translocation pathway and the binding sites for substrate and co-substrate ions. Within the outer scaffold of helices, other symmetry-related helices (the third and fourth of each repeat) form V-shaped elements, that together create a second sub-domain, described as looking like a hash symbol (#) (Fig. 5A) [21]. The conserved 10 TM-helix core of the LeuT fold appears to be the essential component required for transport function, although in some cases this core structure is supplemented by peripheral structural elements common to a specific transporter family.

Almost every structure of this highly conserved protein fold reveals a different conformational state of the alternating access cycle (Table 1, Fig. 1). A Ce state was observed for AdiC [89,92], and for one of the three Mhp1 structures [84], while several structures of LeuT [93–97] and one of Mhp1 [84] show CSec conformations with the substrates bound to a common location approximately halfway across the membrane bilayer, and in the center of the core domain (Fig. 5A and B). Conservation of the substrate location was observed in the alternate states. Specifically, in structures of vSGLT [83], CaiT [86,87], and AdiC [90] with the substrate binding site occluded or accessible from the cytoplasm, the CSic and CSi states were identified, respectively. Additional structures of Mhp1 [21], and CaiT [86,87] reveal open, substrate-free Ci conformations. Two somewhat more symmetrical, occluded structures that nevertheless contain some form of pathway to the cytoplasm: one with substrate bound (CSic, BetP [85]), and an apo form (Cic, ApcT [88]), have also been reported. Although the general location of the substrate binding sites appears conserved, the composition of the residues coordinating the substrates varies significantly. For example, in the Na^+-coupled symporters LeuT, vSGLT, BetP and Mhp1, only one of the two sodium ion binding sites is conserved. In LeuT, the sodium ion at the so-called Na1 site is directly coupled to the carboxy oxygen of the substrates, and is not present in other transporters, whereas the second Na2 site of LeuT appears to be conserved in both vSGLT and Mhp1 (see section 4).

Based on these structures, as well as non-equilibrium molecular dynamics simulations [98] and single-molecule FRET data on LeuT [99], a gating-type model has been proposed to describe the common transport mechanism for the LeuT fold. In this mechanism, gate opening would occur via flexing of the first helix of each repeat in a way that would render the binding sites accessible. Bending of these helices appears to be feasible, based on, e.g., comparison of substrate-free conformations of AdiC with substrate-bound conformations of a high-affinity AdiC mutant [90]. Still, whether such flexing of the first helix of each repeat is sufficient to cause exchange from CSe to CSi remains to be demonstrated. Notably, the fact that binding of tryptophan to LeuT creates a Ce state of the transporter provides a second example of inhibition by trapping of a low-energy state to which the substrate, by contrast, binds less favorably.

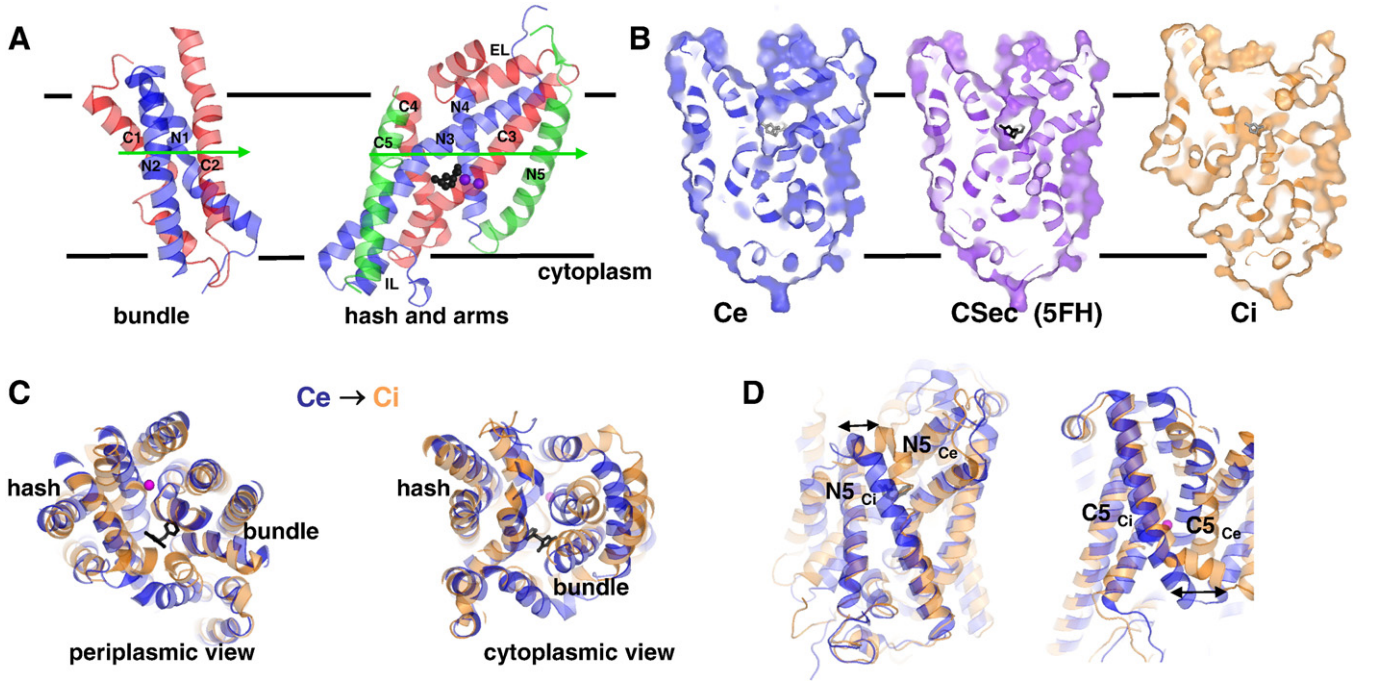

Fig. 5. Overall fold, conformations and substrate binding in LeuT fold carriers. (A) All LeuT fold transporters share a repeated structural motif of five TM helices that have inverted topologies and are closely intertwined. The first two helices of each repeat (N1-N2 and C1-C2) form a four-helix bundle that is surrounded by a scaffold that includes the hash domain (N3-N4 and C3-C4) and two arms (N5 and C5, shown in green). The first five TM helices (blue) are structurally homologous to the second five (red). The two-fold pseudo-symmetry axis, running parallel to the membrane plane, which relates the repeat units is displayed as green arrow. (B) Cross-sections through the three structures of Mhp1 viewed from the plane of the membrane. The three structures are: in the Ce conformation in complex with a sodium ion (PDB entry 2JLN); in the CSec conformation in complex with (5 S)-5-benzylimidazolidine-2,4-dione (5FH), shown in stick representation in black and with one sodium ion (PDB entry 2JLO); and in an Ci conformation (2X79). In the Ce and Ci states the substrate location observed in the CSec state is indicated in grey. (C) The bundle, hash regions and the arms of Mhp1 in the Ce (blue) and Ci (orange) conformations, viewed from the periplasm (left) and the cytoplasm (right). Some loops have been removed for better visualization. The bundle and the hash domain move relative to one another, similar to a rocker-switch mechanism. (D) Side view of the fifth helix of each repeat (N5 and C5) in the Ce (purple) and Ci (orange) conformations of Mhp1, showing the flexing of these helices around their glycine-rich midsections, forming the thin gates.

A second proposal for the major conformational change, more similar to a rocker-switch mechanism, was first put forward based on biochemical accessibility measurements on a mammalian LeuT homolog, and on a molecular model of the CSi state of LeuT created by swapping the conformations of the internally symmetric structural motifs [100] (see also Glt_{Ph}, above). Specifically, the LeuT model suggests that during the conformational switch from CSe to CSi the four-helix bundle (Fig. 5B) would be relatively rigid, and would rock against the scaffold. Such a mechanism inherently allows for coupling of the opening of one side of the pathway to closure of the other side, would maintain the integrity of a chloride ion binding site within the bundle, and is consistent with the fact that the helices in the bundle are connected by very short loops which may limit the relative movements of the helices [19].

Structures of Mhp1 [21,84], which have been solved in Ce (PDB entry 2JLN), CSec (PDB entry 2JLO) and Ci (PDB entry 2X79) conformations (Fig. 5A), and molecular dynamics simulations thereof [21], however, suggest a combination of the two types of mechanism, containing features of both rocker-switch and gating models [22]. Thus, during the main conformational switch, the bundle (along with various peripheral helices) moves relative to the other parts of the structure (primarily the hash domain), similar to a rocker-switch mechanism (Fig. 5B). At the same time, helices connecting the bundle and hash domains (the fifth helix of each repeat) bend and flex at glycine residues near their midpoints (Fig. 5B and C). This flexing aids in the occlusion of the substrate by reversibly folding over the top of the binding site, and thereby these helices act as thin gates (Fig. 5C). Such movements may be limited to the NCS1 family however, since equivalent helix-breaking residues are not found in all LeuT fold transporter families. Unlike the Glt_{Ph} mechanism, the closing or opening of these thin gates does not involve residues that coordinate the substrate in the CSec state. However, small obstructions to substrate release (thin gates) are also observed in the LeuT, AdiC and vSGLT structures, and these are indeed formed by side chains from the binding site. Thus, the LeuT fold presents two types of gating mechanisms by which bound substrate can be occluded.

A crucial question is how the two steps of the LeuT fold mechanism (the domain-rocking movement and the gating movements) are related sequentially. It has been proposed that after substrate binding to the Ce or Ci state, closure of the thin gates (whether side chains or flexible helices) occludes the substrate in the primary binding site, creating the CSec or CSic state [18]. Unbinding would therefore involve the reverse, opening process. The energy cost of such thin gate substrate occlusion events may well be minimal, as the conformational states involved are likely to be sampled due to thermal fluctuations, similar to the observation for the thin gates of Glt_{Ph}.

Subsequent to the occlusion step, the domain-rocking movement (opening and closing of the thick gates) would then be responsible for switching the transporter between the CSe and CSi states. This transition would reorient the entire membrane-spanning bundle of helices along a central axis approximately perpendicular to the membrane, as observed for the transition in Mhp1 (Fig. 5). An advantage of such a pseudo-rigid-body conformational change is that it efficiently synchronizes the opening on one side with the closure on the other side [100]. The energetic barrier to such a large conformational change in antiport and symport, according to the transition state theory of enzymology, must be lowered by the binding of all required substrates, although it is still expected to be larger than the barrier to opening and closing of the thin gates. However, a detailed understanding of which transporter-substrate interactions are essential for changing the energetic landscape in this way, remains elusive.

Recent binding and flux measurements, as well as steered molecular dynamics simulations of LeuT [98] have suggested the presence of an additional binding site, known as S2, in a vestibule between the primary site and the bulk extracellular solution. Based on these data, it has been proposed that the simultaneous occupancy of the two sites triggers the intracellular release of sodium ions and of substrate from the primary site. X-ray diffraction studies of LeuT, however, do not show binding of the substrate anywhere other than the primary binding site, although the Ce conformation of LeuT in complex with tryptophan does bind a second tryptophan molecule at S2 [93], and antidepressants [94,96,97], and detergent molecules [95] have been observed in that exact location, providing interesting examples of non-competitive inhibition. Structural and biochemical studies of CaiT have identified an analogous binding site in the intracellular vestibule [86], as well as a possible cooperative binding site on the extracellular surface that is occupied by either L-carnitine or γ-butyrobetaine [86,87]. The extent and purpose of such allosteric mechanisms remain to be firmly established, since it is also possible that such sites are simply transiently occupied as substrates move towards the primary binding site [18].

In summary, the structural data for the LeuT fold suggests a combination of the rocker-switch and gating-type mechanisms in order to achieve alternating access. In contrast to Glt_{Ph}, it has generally been assumed for the LeuT fold that the substrate binding location is essentially unchanged during transport, consistent with the SBCGP model, although this remains to be demonstrated since the CSe → CSi transition is yet to be described structurally for the same protein.

3.5. Impact of symmetry on fold-specific conformational changes

The topologies of the MCF, MFS, EAAT and LeuT folds appear at first glance to be difficult to compare, due to significant differences in the arrangements of the helices, the lengths of those helices, as well as degrees of bending and unwinding. However, as alluded to above, it turns out that each of the four folds can be subdivided into a number of repeated structural elements (or 'repeats'), which are related to each other by a distinct symmetry axis (Fig. 6). Remarkably, the conformational changes that those proteins undergo all appear to involve symmetry-related movements of those structural repeats. For example, the conformational change described for LeuT by structural

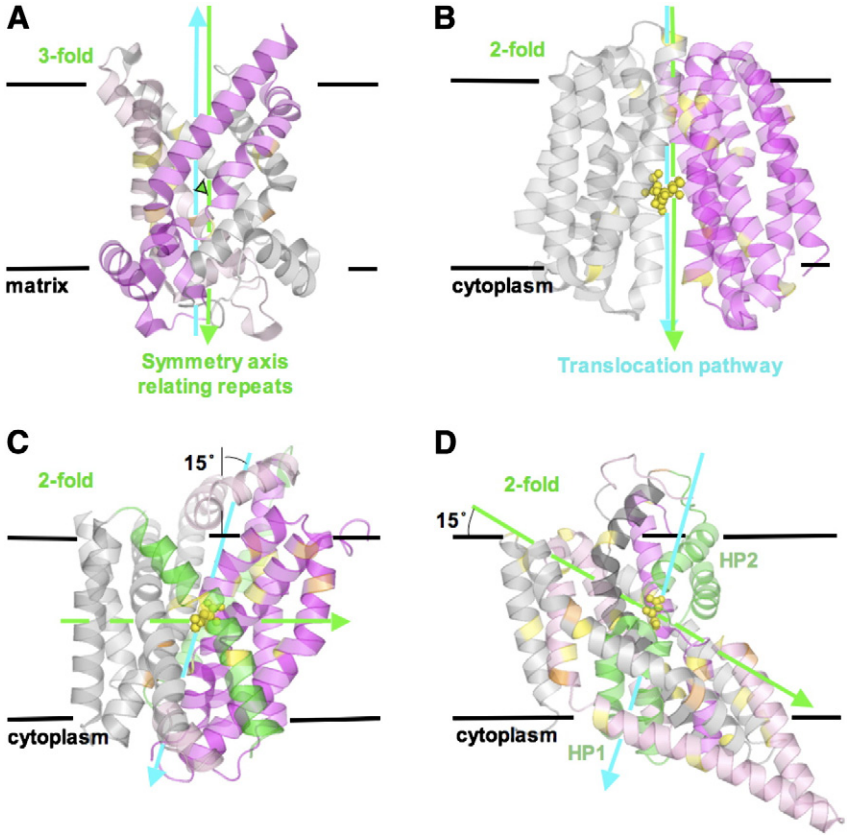

Fig. 6. Symmetry relation between structural repeats in the four secondary transporter folds (MCF, MSF, LeuT and Glt_{Ph} fold) relative to the substrate translocation pathway. In all four structures, substrates (yellow spheres), proline (yellow) and glycine (orange) residues are highlighted, as are the symmetry axis (green arrow) and the translocation pathway (cyan arrow). (A) Side view of the X-ray structure of the ADP/ATP carrier (BtAAC1) in ribbon representation. The three repeats are colored in magenta (repeat 1), grey (repeat 2) and light pink (repeat 3). They are related by a three-fold symmetry axis (green arrow, green triangle) that is perpendicular to the plane of the membrane. The symmetry axis relating the repeats is parallel to the direction of substrate translocation pathway (cyan arrow), which also runs through the center of the carrier. (B) Side view of the X-ray structure of LacY. N-terminal (magenta) and C-terminal (grey) repeats are related by a two-fold axis (green arrow) running through the center of the carrier, parallel to the membrane normal and to the substrate translocation pathway (cyan arrow). While the TM helices of each repeat contain only a few proline residues (orange), the fold is characterized by numerous glycine residues (yellow) at the periplasmic and cytoplasmic ends of each helix. (C) Side view of the X-ray structure of LeuT. TM11 and TM12 have been removed for better visualization. The bundle is shown in magenta, the hash region in dark grey and the two arms in green. Numerous glycines (yellow) and prolines (orange) are found halfway across the membrane-spanning helices. The inverted structural repeats (TM1-TM5 and TM6-TM10) are related by a two-fold symmetry axis (green arrow) running parallel to the membrane plane along the 'glycine belt' in the halfway across the membrane. The translocation pathway (cyan arrow) runs through the center of LeuT but adopts an angle of about ~15° to the membrane normal. (D) Side view of the X-ray structure of Glt_{Ph}. Repeat 1 is colored in light grey, repeat 2 in light pink, repeat 3 in magenta and repeat 4 in dark gray. The hairpins HP1 and HP2 are colored in green. Both inverted structural repeats pairs (repeat 1–2 and repeat 3–4) are related by a two-fold symmetry axis (green arrow) along the 'glycine belt' at an angle of about ~15° from the membrane plane. The translocation pathway (cyan arrow) runs through the center of Glt_{Ph} at an angle of about ~15° from the membrane normal, similar to that observed for the LeuT fold.

modeling could be created by swapping the internal conformations of the inverted-topology repeats in the CSec crystal structure, as mentioned above. Specifically, the sequence of the first repeat was allowed to adopt the conformation of the second repeat, and *vice versa*, and this process led to a model of the CSic state because the inherent differences in the repeats [19,100]. This outcome could also be achieved for Glt_{Ph}, even though its architecture is significantly more complex [78]. Thus, the symmetry in the structure encodes the conformational changes required for transport. However, as will be discussed below, the orientations of the internal symmetry axes that those movements follow differ substantially between structural families.

In MCF and MFS proteins the structural repeats also show sequence homology, providing strong support for the idea that these repeats resulted from gene duplication of an ancestral (carrier) protein [40,48]. In the MCF family, there are three repeats of two helices each, which are related by a three-fold symmetry axis running parallel to the membrane normal, straight through the center of the carrier (Fig. 6A). Residues believed to be involved in conformational changes, i.e., prolines in the signature motif of each repeat, strictly follow the three-fold symmetry. In MFS transporters, the repeated domains are related by a two-fold symmetry axis (Fig. 6B) rather than a three-fold axis, and yet in both MCF and MFS folds, the respective symmetry axis runs along the translocation pathway. Indeed, this coincidence of the symmetry axis and the pathway is clearly well suited to formation of alternating, symmetry-related states. However, the specific conformational changes required for transport are clearly different for proteins with two-fold versus three-fold symmetry. For two-fold symmetry, a rocker-switch (or clamping and releasing) movement of the repeats along their symmetry axis is well suited to opening and closing the central binding site. Primarily rigid-body movements are also consistent with the domains being made up of relatively straight TM helices, with very few significant deviations from α-helicity, containing glycine-rich (bendable) segments only at their extra-membranous ends. By contrast, the three-fold symmetry-related repeats of the MFC proteins have been proposed to undergo an iris-like twisting of the TM helices relative to the short helices on the matrix side [41]. In such a movement, the cytoplasmic and matrix parts of the helices might be able to bend at the pronounced hinge regions in the TM helices that are formed by prolines from the signature motif.

In the LeuT fold the repeats are related by a two-fold symmetry axis as in LacY, but here no sequence homology is observed between the repeats. Moreover, in the LeuT fold the symmetry axis runs parallel to the membrane plane and consequently the repeats have inverted topologies (Fig. 6C). Because this axis runs through the repeats (rather than between them), their helices are interwoven. Nevertheless, together the repeats form two structurally distinct protein domains (the bundle and hash domains). This is in contrast to the MFS proteins, where the axis runs between the repeats and those repeats are largely structurally independent. Another interesting consequence of the inverted-topology of the repeats in LeuT is that the symmetry axis and translocation pathway run nearly perpendicular to one another, while in the MFS fold they run along the same axis. Remarkably, the end effect for these two very different folds (MFS and LeuT) is that the conformational switch probably occurs by the rocking of two domains against one another along an axis that runs perpendicular to the membrane plane. In the case of the LeuT fold this motion arises from rocking of the bundle and hash domains relative to one another, rather than the repeats, and thus the axis of this motion does not run parallel to the symmetry axis as for the MFS fold, but rather along an axis running through the center of the 10-TM core, perpendicular to the membrane plane (Fig. 6C).

In Glt_{Ph} the symmetry relationships are rather more complex [77,78]. Specifically, two independent sets of repeats are related to one another by two-fold symmetry (Fig. 4B), and the symmetry axis is now tilted with respect to the membrane plane, running from the outermost corner of each protomer towards the center of the trimer (Fig. 6D). As for the LeuT fold, the symmetry axis and translocation pathway are nearly perpendicular to one another. Similar to LeuT, the repeat units of each pair have inverted topologies and come together to form two structurally distinct protein domains (transport domain and scaffold). The entire transport domain containing the binding site and both gates (as well as some movement of the adjacent lipid-facing TM helices 3 and 6), translates towards the cytoplasm during the CSec → CSic transition, while the scaffold domain remains more or less static. These relative movements can be interpreted, to some extent, as a rocking motion along an axis that is tilted with respect to the membrane normal, i.e., parallel to the translocation pathway. Moreover, the orientation of external and internal gates is strictly related by the symmetry axis that relates the two inverted-topology repeats.

Finally, we note that elements from both the MFS and Glt_{Ph} folds are found in the LeuT fold. In addition to the two-fold symmetry that is shared by the MFS fold, the gating in the LeuT fold, i.e., occlusion of the substrate binding site, occurs via thin gates as in the Glt_{Ph} mechanism. In some cases, the thin gates contain secondary structure elements as in Glt_{Ph}, and in others the occlusion is formed by individual side chains. In marked contrast to Glt_{Ph} however, the binding site in LeuT does not move during translocation.

3.5.1. Status of the transport mechanism in the remaining folds

We have discussed molecular transport mechanisms for four folds in detail, but what about the remaining four folds, for which such a description was not possible? There are several reasons why structural information available for these four carrier folds did not easily lead into a description of conformational changes that fits within an alternating access mechanism. These include lack of structural data in different conformations, and insufficient resolution in the case that the substrates consist entirely of ions. In the following, we will briefly discuss the limiting factors for each of the remaining folds.

3.6. Sodium-coupled proton antiport in NhaA

The Na^+/H^+ antiporter NhaA has a unique ability for pH sensing and has been studied extensively using biochemical approaches for many years [30,101]. The characteristic feature of the structural fold of NhaA is a pair of discontinuous TM helices with opposite orientations to one another in the membrane, reflecting also the presence of inverted-topology repeats [22,102]. The unwound stretches that cross in the middle of the membrane are accessible from the cytoplasm by a broad funnel and thus the conformation of this structure was assigned to Ci state. A shallow periplasmic funnel to the crossing stretches, separated from the cytoplasmic funnel by a non-polar barrier, was also observed. Moreover, because crystallization was performed at acidic pH, where NhaA is inactive, this structure probably represents an inactivated state of the protein. Thus, together these aspects conspire to complicate the assignment of the state of this structure.

Due to the modest resolution of the data (Table 1), neither substrate could be assigned to the structure, although it has been proposed based on molecular dynamics simulations that the cytoplasmic funnel is accessible to water and hydrated cations, while the narrow periplasmic funnel can only be accessed by non-hydrated Na^+ ions [103,104]. Interesting proposals relating to the activation mechanism, involving e.g., rotation of a helix adjacent to the crossing helices, have also been put forward based on the molecular dynamics simulations [103,104]. Nevertheless, since these simulations are based on a structure of the inactive state at low resolution additional experiments and additional structures will be required to confirm or disprove these findings.

3.7. Multi-drug resistance by EmrE

Two X-ray structures of EmrE from *E. coli*, which is an archetypal transporter of the *small multidrug resistance* (SMR) family have been

solved to 4.5 and 3.8 Å resolution (PDB entries 3B61 and 3B5D [105]). EmrE is an H^+-coupled antiporter that extrudes toxic polyaromatic cations from the cell. EmrE consists of only 4 TM helices, considered to be too small to form an entire transporter unit alone and was therefore assumed to be a functional dimer [106,107]. Indeed, a dimeric arrangement was observed in a 7.5-Å cryo-electron microscopy map of EmrE, which displayed a physiologically unusual asymmetry [108]. A structural model generated for this map guided by conservation analysis [109] agrees remarkably well with the X-ray structures mentioned above [105]. In these structures, the protomers are oriented antiparallel in the membrane. The physiological relevance of the antiparallel dimer is a matter of some controversy, as there is support for a parallel configuration from biochemical and spectroscopic studies [110,111]. Nevertheless, there is general agreement that EmrE can insert into the membrane in two opposing orientations at the same time [112] (i.e., it has two different topologies), which is a novel and remarkable architecture for a secondary transporter.

The proposed substrate binding site, which consists of aromatic and negatively charged residues, is located at the dimer interface. Interestingly, in both orientations the substrate binding site would be expected to contain a perfect two-fold symmetric distribution of residues, a unique property of homodimeric proteins, such as the SMR transporters.

3.8. Proton-dependent multi-drug efflux by AcrB

AcrB, a member of the *resistance nodulation cell division* (RND) family from *E. coli*, is part of a three-component system together with AcrA and TolC that is responsible for transport of noxious substances such as dyes, detergents, bile salts and antibiotics out of the cell. AcrB is responsible for the drug specificity and energy transduction in this tripartite system [113,114]. Unlike the secondary transporter structures discussed in the previous sections, the AcrB protomer contains, aside from its membrane components, two large periplasmic segments that comprise the TolC docking domain. Its structure has been solved in a three-fold symmetric conformation but also later in an asymmetric conformation, which is thought to represent the physiologically relevant form [113,115].

The AcrB protomers in the asymmetric trimer structure [116,117] were suggested to represent consecutive steps of a transport cycle. However the terminology of outward- or inward-facing state of the alternating access was not attributed; instead the three states were designated as loose (L), tight (T) and open (O), which reflects the formation of several different tunnels connecting TolC with the membrane outer leaflet. One reason for this different assignment is that, unlike the classical alternating access mechanism, the substrate and counter-substrate (protons) for AcrB are recruited from different compartments. That is, while the drugs bind from the outer leaflet of the membrane and are released into the periplasmic funnel formed by TolC, protons bind from the periplasm and are released to the cytoplasm. Hence, there is no common substrate binding site that is accessible from one side of the membrane during transport. The proposed cycling mechanism in fact resembles more closely that of a peristaltic pump, with analogies to the mechanism of ATP synthesis by the F-ATPase [116]. Therefore, description of conformational changes in the AcrB antiporter does not easily fit into a general alternating access mechanism.

3.9. Chloride conductance and transport by CLC proteins

EcClC from *E. coli* is a bacterial homologue of the *chloride channel and transporters* (CLC) family. It has been shown that this bacterial homologue is not an ion channel, but functions rather as a Cl^-/H^+ antiporter [118]. This remarkable finding suggests that the structural boundary separating channels and transporters is not as clear-cut as previously thought [119]. The structure of this homodimeric transporter exhibits a complex topology, with two structurally related inverted-topology halves within each protomer [120]. The Cl^- translocation pathway is an hourglass-shaped pore, located at the interface between the two halves of each protomer, containing a selectivity filter formed by OH groups of one serine and one tyrosine side chain as well as amide NH groups of the protein backbone at the constriction. Two of three binding sites were occupied by chloride ions in the structure of the wild-type protein, and occluded at the third (extracellular) binding site by the side chain of a conserved glutamate residue Glu148 [120]. It has been suggested that the conformations of the aforementioned tyrosine and serine side chains coordinating the second chloride binding site constitute an intracellular gate, which prevents free exchange of the ion with the cytoplasm, and would therefore correspond to an occluded CSic state. However, an assignment to a defined conformational state during the alternating access cycle is not trivial. The transported chloride anions move along a preformed pathway in this transporter similar to the way they would in ion channels, and the relatively fast transport kinetics (which were estimated to be on the microsecond time-scale), suggests no large conformational changes other than the movement of the glutamate side chain to the third binding site of chloride [121,122].

4. Coupling in secondary transport

4.1. Uniport, symport and antiport mechanisms require different sets of rules

The concept of coupling of the free energy of the electrochemical potential of one solute to the transmembrane movement of another is integral to a discussion of mechanistic differences between uniport, symport and antiport mechanisms in secondary active transport. In this framework, coupling is described on a formal level by a set of rules [11,16]. For coupled secondary transport, the underlying rule is simply that transport of the substrate is allowed to occur only when the co-substrate is also transported. More specifically, in kinetic schemes similar to Fig. 1, the switch from the e (=external) conformation of the transporter to the i (= internal) conformation is allowed for some intermediates or complexes, but forbidden for others (Fig. 7). In a strict antiport system, such as the mitochondrial ADP/ATP carrier, the binary complexes with either ADP or ATP are

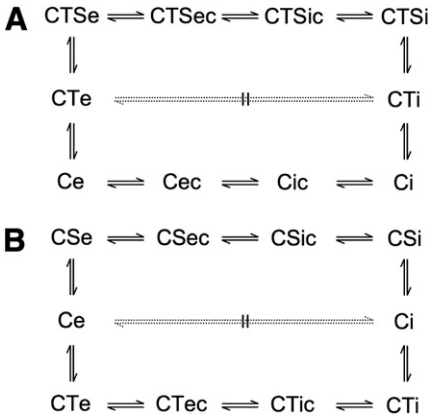

Fig. 7. Carrier model for a symport and a strict antiport mechanism. C is the carrier protein, S and T are substrate and co-substrate, respectively. The subscripts indicate the respective carrier conformations e, i, and c, for externally and internally exposed, and occluded state. Broken connecting lines indicate a 'forbidden' step in the cycle. (A) Symport is shown in a symmetrical ordered mechanism. In the binding order of co-substrate and substrate, T is first and S is second. For transport of T and S to be coupled, the CeT↔CiT transition is forbidden. Unidirectional uptake in the symport mode involves the whole cycle, whereas exchange (and counterflow) of substrate would only require the upper half of the cycle. (B) In strict antiport of the two substrates T or S, the Ce↔Ci transition is not allowed to occur.

allowed to switch, whereas the empty carrier is not. For a symporter, such as LacY, a conformational switch is allowed in the ternary form, i.e., with both substrate (lactose) and co-substrate (proton) bound, as well as for the empty carrier, while the binary complexes are locked. These rules are able to describe how uncoupling of a coupled vectorial process is prevented, but the structural basis of these coupling rules is only now beginning to be understood. We wish to describe, for example, which structural properties define the ability of a particular bound state of a transporter to undergo the conformational Ce↔Ci switch, and why this depends on the type and number of bound substrate ligands.

In the following, we will address the mechanisms of first antiport, and then symport, and consider, in each case, which energetic and kinetic characteristics are associated with the aforementioned rules. Note that this mechanistic discussion requires a clear distinction to be made between the nature of the carrier protein itself, and environmental factors such as substrate concentration gradients and the membrane electrical potential.

4.2. In antiport, substrate binding provides the energy for the major conformational change

If the above formal definition of rules is combined with the concept of induced transition fit (see section 2), the mechanism of antiport, which is the simplest form of coupled transport, is particularly easy to understand. This is because in both 'inward' and 'outward' directions, the catalytic energy necessary for effective substrate translocation, i.e., for lowering the activation energy barrier for the conformational change of the carrier protein, is provided in both directions by the intrinsic energy of substrate binding at the appropriate side of the membrane. The only requirement in terms of coupling is that there is not enough catalytic energy available to allow interchange between the Ce and the Ci conformations of the carrier in the absence of bound substrates, implying a very high activation energy barrier for the conformational change of the empty carrier (Fig. 7). Thus, the direction of antiport, i.e., the extent to which each of the substrates is transported in a given direction, depends simply on the concentration ratio of the two substrates corrected for their affinities to the binding site.

4.3. Antiport of charged species affects, and is affected by, the membrane electrical potential

Even for antiport the mechanism becomes more complicated if the two antiport substrates differ in charge. Under these conditions, transport becomes influenced by an electrical (membrane) potential. The best studied example of this effect is counter-transport by the mitochondrial ADP/ATP carrier, which, under energized conditions of mitochondria in the presence of a high electrochemical potential, favors the export of ATP^{4-} out of mitochondria in exchange for import of ADP^{3-} into mitochondria, along the membrane potential, i.e., with positive polarity outside [123]. Another well-described example is substrate/product antiport in bacteria [124], which frequently involves substrates with different charge states. The role of the membrane electrical potential in secondary transport is discussed in more detail in the context of symport mechanisms (see below).

In the case of the ADP/ATP carrier, the differently charged species become accumulated in a way that diminishes the mitochondrial membrane potential. In the case of precursor/product antiport, by contrast, asymmetric substrate movement driven by their chemical potentials (opposing concentration gradients of two differently charged substrates) actually generates a transmembrane electrical potential. An interesting recent example of the latter mechanism is exhibited by the AdiC protein [89], for which 3D structures were recently reported [89,92]. AdiC catalyzes the exchange of external arginine for its cytosolic decarboxylation product agmatine, effectively resulting in the export of protons, and concomitant generation of a membrane potential. In the light of these examples, the energetic equivalence of the two components of electrochemical potentials, namely the chemical and the electrical components, becomes clear. That is, for the ADP/ATP carrier the electrical component drives formation of the chemical component, while for AdiC the chemical component drives formation of the electrical. An understanding of this equivalence is instrumental for our discussion of driving forces in coupled symport mechanisms.

4.4. Symport requires the empty carrier also to change conformation

An attempt to explain symport mechanisms in the conceptual framework used above, however, introduces new challenges. This is because, in unidirectional transport, irrespective of whether it is coupled to the gradient of a co-substrate (symport) or not (uniport), the return of the carrier protein to the initial ground state requires a conformational change of the empty protein from Ci to Ce, or *vice versa* (Fig. 7). Remember that, in the case of strict antiporters, such a step must be forbidden, i.e., characterized by a very high activation energy barrier. This raises the question of what property makes the energetic barrier of this step sufficiently low that it is accessible without the aid of substrate during symport. In some cases, catalytic energy for this step might be derived from the transmembrane potential (see section on membrane electrical potential, below). Another possibility is that the intrinsic energy from the ligand binding step is stored in some way, and then utilized in this part of the cycle. Alternatively, the structural features of symporter proteins may differ from those of antiporters in a way that allows for an inherently low activation energy barrier and thus allows stochastic Ce↔Ci exchange under physiological conditions.

The kinetic difference between Ci↔Ce exchange of the empty and the substrate-loaded carrier becomes obvious in the light of a simple observation. Specifically, in symporters where it has been studied, such as the glucose carrier from erythrocytes [125], substrate antiport has also been detected. Importantly, this basically unproductive form of catalytic activity is, in the presence of sufficiently high substrate concentrations on both sides of the membrane, faster than the productive, physiologically relevant, unidirectional transport function. The obvious explanation for this rate change is a lower activation energy barrier for substrate antiport because of the energy provided by binding of the substrate in the reorientation step of the catalytic cycle.

4.5. Ce↔Ci exchange and the rate-limiting step in symport

The observation of substrate exchange by symporters also suggests that the rate-limiting step (i.e., that with the highest activation energy) in the complete, physiologically relevant symport cycle is found in the later stages of the kinetic cycle (Fig. 7). One possibility is that the conversion of the empty carrier from the Ci to Ce state is rate-limiting. Thus, even though the energetic barrier for this event is lower than during antiport, it may still have the highest barrier of all the steps in the cycle. From a structural perspective, the Ce↔Ci conversion is also the most likely candidate for the rate-limiting step, since it requires the largest conformational change. However, substrate dissociation is also a possible candidate for the rate-limiting step in symport.

In fact, under specific conditions, defined by the substrate and co-substrate concentrations or by the membrane electrical potential, another step in the cycle such as substrate dissociation may, in practice, be slower than the theoretical rate-limiting step for the carrier. There are examples of the two aforementioned situations among structurally and biochemically well-characterized systems. For the intestinal Na^+/glucose cotransporter SGLT1 [126], a homolog of the structurally characterized vSGLT protein [83], analysis of steady-state and presteady-state currents using electrophysiology

[127] have identified two different steps as rate limiting. Thus, the rate-limiting step is either substrate or co-substrate binding, or translocation of the empty carrier, depending on the concentrations of the two substrates and on the membrane potential. For LacY, the H^+/lactose cotransporter from *E. coli*, evidence has been provided that dissociation of co-substrate protons from the cytoplasmic side of the carrier may become a rate-limiting step under specific conditions (see below).

Now that we have described the kinetic implications of the coupling rules imposed during symport, we can begin to consider the consequences of those rules in terms of, e.g., the order of co-substrate binding, or the nature of the binary complex (i.e., with only one substrate bound). Again, we use LacY [28] as an example symporter, because, even though the mechanism of coupling is still poorly understood on the molecular level, a wealth of pertinent biochemical, biophysical, and kinetic data is available.

4.6. Binding of co-substrates in symport is interdependent and ordered

In considering the binding of substrates during symport, it is important to note that the different substrates of LacY, and of secondary transporters in general, do not react with the protein independently from one another, but that substrate binding and release in most cases follow an ordered kinetic mechanism. Indeed, it has been pointed out that this represents one of the few instances in biochemistry in which such an ordered mechanism is essential for the successful functioning of an enzyme [16]. Moreover, thorough analysis of kinetic considerations indicates that a binding order in which the driving substrate (e.g., protons for LacY and Na^+ for SGLT1) is "first on" during loading, and "first off" during unloading, actually minimizes the extent of uncoupled reactions in the catalytic cycle [11]. In the case of LacY, where the binding order at the periplasmic site has been established, the proton does indeed bind before the lactose substrate, but dissociation instead occurs in the reverse order [128]. It can therefore be assumed that binding of lactose requires prior protonation of specific charged residues, most probably E269 and H322 [28,129], or, as suggested by the authors, binding of a hydronium ion to these residues [71]. In mutagenesis studies it has also turned out that binding and transport of one of the substrates cannot be altered without affecting the properties of the other. As will be discussed below, from a structural perspective this can result from one of two situations. Either the coupling ion (Na^+ or H^+) interacts with the substrate, and therefore contributes to the binding site directly, or the ion causes an allosteric change in the structure (or structural ensemble) of the protein as a whole, and thereby indirectly allows formation of the binding site.

4.7. Prevention of uncoupling during symport

To prevent uncoupling, binding of just one of the two substrates must necessarily lead to the formation of a 'locked' state of the carrier that is statistically unlikely to undergo the translocation-related conformational switch. We note that in the course of the extensive mutational analysis of LacY, interesting mutant forms have been identified that exhibit both possible variants of an uncoupled phenotype, namely (i) that catalyze lactose transport uncoupled from proton translocation, and (ii) that allow proton flux uncoupled from lactose transport [130–133]. The binary complexes of these mutants therefore apparently have a much higher statistical probability of undergoing the conformational switch than the binary complexes of the wild-type protein. Remarkably, these observations suggest that single amino acid side chains can govern the coupling rules of a given transporter. It would be of great interest to obtain structural information for these mutants, as this may unveil the structural correlates for the rules that govern locking and unlocking of specific steps in the cycle [11,132].

4.8. The role of the membrane electrical potential in symport

An interesting question relating to coupled transport is how electrical potentials can be included in the mechanistic concept, or, in other words, how the membrane potential imposes directionality on secondary active transport. Again, LacY and SGLT1 provide useful examples on which we can base our discussion. For SGLT1, the membrane potential was found to exert a significant influence on only one step in the catalytic cycle, namely the translocation of the empty carrier, although it also has a minor effect on Na^+ binding to the extracellular binding site [127]. All other steps were found to be independent of the membrane potential.

In proton-coupled transport by LacY, the role of the membrane potential and the question of the rate-limiting step is more complex. A number of results indicate that, although protonation or deprotonation are not rate limiting for either for active transport driven by the electrochemical proton potential or for lactose exchange (see Fig. 7), they do seem to be rate-limiting during passive, proton-coupled efflux of lactose driven by its own gradient [28,134,135]. In addition, kinetic measurements reveal that $\Delta\Psi$ and ΔpH (i.e., the two components of the electrochemical proton potential) both have a strong and equivalent effect on the apparent substrate affinity K_m in LacY, that is, the rate of transport [136]. Finally, electrophysiological measurements confirm that a late step in the reaction cycle of LacY, such as co-substrate release or carrier reorientation, is connected with the energetic input of the membrane potential also under conditions of substrate-gradient driven lactose efflux [137,138]. Based on these observations, Kaback and colleagues have suggested that deprotonation of LacY at the cytoplasmic face of the transporter is not only the rate-limiting step in the transport cycle, but also the particular kinetic step that is modulated by the electrical potential [28,129,137,138]. That is, a high membrane potential is proposed to accelerate deprotonation of CHi, which would increase the population of the Ci state (Fig. 7A), and this in turn would increase the probability of empty LacY to switch from the Ci to the Ce state. Taken together, the evidence suggests that, at least under specific conditions, a step other than the reorientation step can indeed be the rate-limiting step, and furthermore that the deprotonation step at the cytoplasmic face of the protein is the partial reaction within the cycle that is influenced by the membrane potential.

The question remains, however, how in this model the electrical potential can change the affinity of the co-substrate binding site, which, for LacY, would mean changing the pK_A of the proton binding site that is exposed in the CHi configuration. One possible explanation of the influence of the electrical gradient is that it depends on the net charge of the carrier itself. In particular, for the potential to affect the least efficient step (presumably reorientation of the empty carrier), we can assume that the empty transporter, but not the ternary complex (with lactose and protons) carries a net negative charge that is capable of sensing the electrical potential. Thus, the electrophoretic impact of $\Delta\Psi$ (positive outside) would be to provide the catalytic energy necessary to increase the efficiency of the reorientation step in the translocation cycle [139]. Although this concept would in fact provide a mechanistic explanation for a direct influence of electrical potentials on the transport cycle, no structural information in support of this mechanism is currently available.

Having now described the implications of coupling rules in both kinetic and mechanistic terms, we can proceed to consider what the recent structural and dynamic insights from crystallographic and computational studies reveal about the molecular counterparts of these theoretical and empirical observations. We will first address sodium-coupled transport from two different structural folds (LeuT and Glt_{Ph}), for which sufficient data is now available for a detailed description. This will be followed by a brief discussion of proton-coupled transport, including for LacY.

4.9. Ion binding and coupling in transporters of the LeuT fold

The X-ray crystal structure of LeuT, first solved at 1.65 Å resolution, provided the first detailed insights into the interactions of the coupling ions to any secondary transporter [82]. Although the electron density of sodium is indistinguishable from that of a water oxygen, the nature of the coordination in the structure [82], comparison with biochemical data [140–143], and subsequent computational analyses [98,144–146] together provide convincing evidence for two sodium binding sites in LeuT, which turn out to be rather distinct in their nature.

The first of the two sodium binding sites, Na1, remarkably, includes the amino acid substrate itself, which directly coordinates the ion through a backbone carboxylate oxygen atom [82]. Such a direct interaction allows a satisfying molecular description of coupling in which the binding affinities of the substrate and ion are inexorably co-dependent. Support for this concept has been provided by molecular dynamics free energy calculations [98,145], which also suggest that Na1 is a rather high-affinity site [98,144]. Together these data indicate that the electrostatic component of the interactions is the primary requirement in ion-based coupling in LeuT, although coordination (van der Waals) and desolvation effects will obviously also play some roles [144].

The second site for sodium in LeuT, Na2, is separated from Na1 by one transmembrane helix (TM1) and is located slightly more towards the cytoplasm than the substrate binding site. Thus, although direct coupling to the substrate does not occur for this ion, the presence of the substrate occupying the extracellular pathway may provide a means of coupling by inhibiting re-release of the ion [21].

At Na2, the sodium ion is coordinated by polar groups from the protein backbone, as well as by side chain hydroxyl groups [82]. Equivalent side chains have also been identified by biochemical and structural studies as probable binding sites in other sodium-coupled transporters of the same fold, including vSGLT [83], sodium-iodide symporter [147], γ-amino butyric acid transporter GAT-1 [140], BetP [84,85] and Mhp1 [84], suggesting a common sodium binding site [18,20]. Remarkably, structures of the ApcT and CaiT proteins reveal that the electrostatic component of monovalent cation binding to Na2 may be mimicked by a basic amino acid side chain, which may remove the ion requirement in antiport by CaiT [86,87], and possibly also introduce proton coupling in the case of ApcT [88]. Thus, the electrostatic component appears to be the most critical feature of the ion-protein interaction also at this second binding site in the LeuT fold.

Together these observations suggest that the LeuT fold architecture contains a common requirement for interactions at the location of Na2. In fact, assuming that a rocker-switch-type conformational change (involving relative movements of the bundle and the hash domain) connects CSi and CSe, the Na2 site is situated precisely at the nexus of the two major moving parts of the protein, providing direct interactions to both the bundle (TM1) and the hash domain (TM8) that may enable it to directly modulate the conformational change [19,100]. Further support for this proposal comes from biochemical studies of an NSS transporter, which indicate that sodium binding to Na2 results in changes in accessibility of TM1 [148].

Interestingly, the Na2 ion in the CSe state of LeuT has been calculated by free energy perturbation molecular dynamics simulations to have a relatively weak binding affinity [98,144]. By contrast, more qualitative molecular dynamics simulations [21,149], as well as the fact that the coordinating groups are relatively distant from one another in the structures, indicate that in the CSi or Ci conformations reported for vSGLT [83] and Mhp1 [21], respectively, this sodium binding site is essentially not intact. These observations raise an interesting conundrum since it is presumed that the substrates must bind efficiently to both inward- and outward-facing conformations of the carrier in order for a symmetric (reversible) symport process to be possible. This discrepancy might be explained by assuming some plasticity in the CSi/Ci states (i.e., a large conformational ensemble), so that as the domains move closer together, the ion may bind and then facilitate the full transition to the Ce states.

For ApcT, it has been proposed that protonation and deprotonation of a lysine at Na2, may also modulate the conformational change, by analogy with sodium binding and unbinding [88]. Specifically, in the known Cic structure of ApcT, this lysine residue is predicted to be deprotonated, and the local interactions with surrounding Na2 residues are minimal. Upon protonation, however, the charged side chain might optimize the local interactions with TM1 and TM8 akin to the observed sodium–ion coordination in LeuT, thereby directly modulating the conformations of these helices by the electrostatic properties of the side chain, and leading to formation of the Cec state. Presumably, the relatively rigid nature of the bundle and hash domains [21] allows for those local conformational changes to be translated into the full transition to the other state.

Finally, aside from their sodium dependence, eukaryotic members of the NSS family also have a strong dependence on chloride. Studies inspired by sequence analysis, and by calculations of the electrostatic potential of the available structures, suggest that this requirement is also primarily electrostatic. Specifically, the chloride dependence can be replaced biochemically by the introduction of an acidic side chain as found in chloride-independent prokaryotic homologs such as LeuT [150,151]. Interestingly, the acidic side chain introduces an additional requirement for the bacterial transporters, namely for proton counter-transport, so as to neutralize the charged residue while the protein reverts to Ce from Ci [151]. Although two similar and plausible structural models of the chloride binding site in the eukaryotic NSS transporters have been proposed [150,151], confirmation of the binding site location and the nature of its interactions will require further evidence from biochemical and structural studies.

4.10. Ion binding and coupling to glutamate transporters

For the EAAT family of transporters there is also structural evidence for two cation binding sites, which, again, are rather distinct from one another [76]. This evidence was obtained from thallium replacement studies rather than direct evidence of sodium binding, although recent evidence suggests that thallium replaces sodium in many of its key roles [152]. The first site, Na1, is buried deep in the transport domain (Fig. 4), and includes coordination by a conserved glutamate residue [76,153], as well as residues from TM7 and the thin intracellular gate HP1 [79]. In contrast, the second proposed site, Na2 is located between the tip of HP2 and residues in TM8, very close to the aqueous solution (Fig. 4), and is formed only by backbone carbonyl atoms, making it difficult to confirm by mutagenesis. Nevertheless, molecular dynamics simulations suggest that sodium ions are reasonably energetically favored in both these sites [80,154].

Nevertheless, glutamate transport requires symport of three, not two, sodium ions, raising the question of where the third ion might bind. There have been numerous proposals for this site [79,155–157], although the strongest evidence points to two alternatives. The first, which has been named Na3′ is coordinated by an aspartate residue from TM7, and has support from biochemical, electrophysiological [154,155] and computational studies [154,157], although it has been suggested that this site cannot be bound simultaneously with the Na1 site (which is adjacent), and thus perhaps it is only transiently occupied [154]. The second proposed site, Na3, identified by theoretical approaches [154,156] and supported by electrophysiological and fluorescence measurements [154] is coordinated in part by the substrate (glutamate) carboxylate groups, and thus would provide a simple explanation for direct coupling, similar to the role of Na1 of LeuT. A direct ion–substrate interaction would also explain the interdependence of ion and substrate specificity observed for neuronal EAAT transporters [158]. Finally, computational studies have also provided a molecular description of the order of extracellular substrate binding to

the glutamate transporters, integrating the role of the extracellular gate, and supported by evidence from electrophysiological studies [159]. Specifically, it has been proposed that in the apo state, in which HP2 tends to be open, one sodium would enter to the deep Na3′ site, after which Na3 would bind, followed by substrate, reflecting their co-dependent binding nature. Once bound, the substrate would alter the affinity for the ion bound to the deep Na3′ site so that it moves into the Na1 site, which has a more favorable binding energy under these conditions [154]. Importantly, binding of substrate, through direct interactions would increase the probability that the extracellular HP2 gate is closed, thus creating the Na2 binding site [160]. However, only upon binding of the third (chronologically) sodium ion to the Na2 site would the gate be completely closed [80,154]. Complete closure of the thin gates, as mentioned above, is presumably the main requirement for allowing the major CSec ↔ CSic transition of the Glt_{Ph} fold. Thus, by regulating the thin gate closure, as well as one another's binding affinities, the substrate and the sodium together enforce many of the coupling rules for co-transport by this family of transporters.

Thus, structural, biochemical and computational studies have together led to important gains in understanding of the molecular details of coupling by glutamate transporters. Similar insights will now be required for intracellular gate (HP1) opening, and cytoplasmic substrate release, as well as the subsequent re-conversion of the transporter to the extracellular states. Differences between the prokaryotic transporter Glt_{Ph}, for which the Ci → Ce conversion can occur in the empty state, and the eukaryotic EAATs, which instead require potassium counter-transport, will be of particular interest. Such insights may help to explain why transporters of the same architecture can have such different energetic barriers in a given step in the transport cycle, which lead to their categorization as symporters instead of antiporters, or *vice versa*.

4.11. Proton coupling

Structural insights into proton-dependent coupling are clearly more difficult to obtain than for other ion-dependent modes, given the resolution of protein crystallography data currently accessible (~2 Å). Nevertheless, the structural data at least indicates which ionizable residues in the protein are likely to interact with protons, and which might be involved with substrate binding. In FucP, for example, only two ionizable side chains are found in the substrate pathway. One of these has been proposed to be protonated in the inhibitor-bound Ce structure based on molecular dynamics simulations, whereas biochemical assays suggest that protonation of the second side chain is required for substrate binding [54].

For LacY, all available structures appear to be in the protonated form, potentially because they were all determined at pH levels lower than the pKa for sugar binding, which is 10.5 [72]. Nevertheless, in those structures it is possible to identify several ionizable residues in the C-terminal 6-helix bundle, located approximately in the center of the molecule opposite the sugar-binding site (Fig. 3D), which are proposed to play a key role in H^+ translocation [28,128,129,161,162]. One of these residues (Glu269), as part of a wider salt bridge network, can also form a salt bridge with an arginine (Arg144) from the lactose binding site, providing a direct connection within the protein between the two sites that may facilitate coupling of their binding (Fig. 3C). Indeed, the formation of this salt bridge is proposed to correlate with substrate binding, whereas the same residues may form alternate salt bridges with neighboring residues in substrate-free and outward-facing states [28]. The fact that these salt bridge networks also connect the two terminal domains of the protein provides some hints of the way in which binding of protons may couple to the conformational change. Nevertheless, detailed molecular mechanisms coupling proton and substrate binding to one another, and to conformational changes in LacY, remain rather speculative.

4.12. An exception to the rules: Antiport meets channel

The ClC Cl^-/H^+ antiporter from *E. coli* is a fascinating system, not only in its structure (see section 3), but also with respect to its transport function. It represents a remarkable exception from the general 'rule' described in the major part of this review. Since both the structure and function of EcClC is fundamentally different from the other classes of transporters, much can be learned about the basic concept of secondary transport from a thorough comparison of this individual with the rest of the carriers [119,121]). A kinetic analysis of EcClC would not give rise to any major suspicion of its unusual nature, since its function is tightly coupled antiport with a stoichiometry of 2 Cl^- ions exchanged for one proton [118]. However, EcClC is unusual in several ways. In terms of structure, the most obvious difference of EcClC to other secondary carriers is the presence of a channel-type pathway. Chloride anions move along a preformed pathway in a single file movement, consecutively occupying the three Cl^- binding sites. Cl^- is bound to a central binding site in dehydrated form [122], as if in a selectivity filter of a channel. Furthermore, unlike secondary antiporters in which the two substrates use the same pathway through the protein, Cl^- and H^+ appear to travel along different, channel-type pathways through ClC, although the proton pathway has not been resolved structurally. There are also a number of basic mechanistic aspects by which EcClC differs from a typical secondary antiporter. Antiporters bind their substrates alternately in the two different states and shuttle them across the membrane in ping-pong like conformational changes according to the alternating access model. In contrast, ClC is able to bind both its substrates simultaneously, and, importantly, proton movement along its pathway seems only to be possible when the central anion binding site is occupied by Cl^- [118]. Apparently, carrier-type antiport function and substrate coupling are imposed on the channel-like ClC protein by the following features: two glutamate residues at the entrances of the substrate pathway that gate the movements of both H^+ and Cl^-; two separate pathways for H^+ and Cl^- [163,164]; and finally the presence of internal binding site(s) that coordinate the functionally coupled movement of the two substrates.

Consequently, we learn from EcClC that the function of coupled secondary transport can be achieved also by a construction fundamentally different from those of the rest of the carrier systems, that is, using the basic protein machinery of a channel. As long as exclusive alternating access of central substrate binding site(s) is guaranteed and as long as a molecular mechanism is available that functions according to specific rules of coupling, the result is coupled antiport with a kinetic behavior surprisingly similar to 'normal' antiport carriers. Thus, whereas the basic rule of coupling in typical secondary antiporters requires that the Ce↔Ci transition in the absence of bound substrate is not allowed, in the case of EcClC the basic requirement is a channel equipped with two gates carrying central binding site(s) to which one substrate (proton) will bind only when the corresponding site is already occupied by the other (Cl^-).

In summary, the latest structural data, supported by biochemical and computational studies, provides evidence for a number of different molecular mechanisms by which the binding of secondary transporter co-substrates becomes coupled. For example, coordination of one substrate by another provides a direct interaction that imposes co-dependence on their affinities. More long-distance effects appear to arise from electrostatic interactions, such as for chloride stabilization of sodium binding. Finally, steric inhibition, such as by the hydantoin in the pathway in Mhp1, may also modulate co-substrate unbinding and thus enhance its affinity.

Very recent studies also suggest, in microscopic detail, ways in which the substrates or co-substrates can modulate conformational changes in the carrier protein itself, and therefore dictate the rules of coupling for symport or antiport. These include: direct constraints on the thin gates as in the case of ion and substrate interactions with HP2

of Glt_{Ph}; modulation of the major conformational switch by the second cation site in the LeuT fold; as well as the disruption of specific salt bridge networks, as in the case of LacY. Emerging from these data, then, we begin to see a diverse set of solutions that carrier proteins have evolved in order to solve the requirements of coupling in secondary active transport.

5. Conclusions and perspectives

Secondary transport systems are fascinating molecular machines in several aspects. They are perfect little energy converters transforming electrochemical energy into vectorial movement, and *vice versa*. In the history of research on membrane-bound transporters, several phases can be perceived: first a conceptual one in which, for example, the alternating access model was proposed; this was followed by a biochemically active period defined by numerous kinetic, biophysical and biochemical investigations on carrier function; finally, very recently, a structural one, leading to the discovery of an increasing number of 3D and 2D structures of these transporters. This recent development has been supported and complemented substantially by the application of sophisticated computational studies, which allow the information provided by X-ray structures and by biochemistry to be extended and explained. It is the main focus of this review to point out that it should now be possible to close the circle and turn to a new conceptual age in which the combined knowledge of these proteins provides a basis for testing, modifying and finally verifying fundamental concepts of transport.

In spite of the stimulating situation in which we find ourselves, it is obvious that we still have far to go to reach the goal of a complete understanding of the mechanics of transport proteins and, in particular, of coupling in secondary transport. What are the main obstacles to reaching these goals? On the one hand, there are a number of rather basic limitations. For example, we urgently need more structures of individual carriers in different conformations. More precisely, we are looking not only for transporters for which structures of both Ce and Ci states are available, e.g., in the case of LacY, as well as occluded and open states, but also for structures of carrier proteins in as many different states as possible with respect to binding of substrates and, in particular, co-substrates (ions). On the other hand, even though the availability of protein structures of a number of carriers has significantly improved our understanding of the mechanism of secondary transport, we urgently need higher resolution in most cases to allow for unequivocal description of conformational events and, in particular, for accurate descriptions of binding sites. Unfortunately, it may be difficult to overcome these resolution limits because of inherent problems, at least in some cases. It is quite possible that the characteristic properties inherent to carrier-type membrane proteins limit the resolution that X-ray crystallography may bring: Secondary transporters are in general highly flexible proteins with rather small hydrophilic surfaces for appropriate crystal contacts. Beyond the availability of numerous transporter structures with sufficiently high resolution, we will also urgently need the continued support of solid data arising from the application of tried and tested biochemical techniques. There are numerous areas where these techniques continue to be extremely helpful and can help compensate for insufficient resolution in structure. Sophisticated kinetic analysis allows, for example, for a definition of the binding order of substrates, which is essential for accurate descriptions. Similarly, elaborate cross-linking or molecular scanning techniques can provide information on dynamic aspects of neighboring residues.

Probably the most significant barrier to a complete mechanistic picture of secondary transport is the lack of understanding of the molecular mechanisms of coupling, from several perspectives. First, we are still far from a true mechanistic understanding of coupled substrate and co-substrate movement, except for strict antiport systems. In some cases this is due to the lack of structures of sufficiently high resolution harboring bound co-substrate ions. In other cases it is due to the inherent difficulty of localizing protons as co-substrates. Second, we would like to understand how the electrical potential contributes to the directionality of secondary transport beyond a simple picture of the electrogenic movement of a charged carrier complex, and moreover, how the equivalent effects of $\Delta\Psi$ and ΔpH on transport may be explained mechanistically. Third, we are far from understanding substrate/co-substrate stoichiometry and the reasons why it can vary in closely related carrier proteins, or even single-residue mutants. Nothing, for example, so far explains why two closely related glycine transporters couple different numbers of sodium ions to the transport of a single substrate [165]. Finally, we wish to know more about the structural correlate of the fundamental 'rules of coupling' in the different systems. It would be attractive to understand mechanistically, why, for example, the empty carrier in antiport systems is not able to undergo the Ci↔Ce transition, whereas in structurally similar symport systems this transition is allowed.

In conclusion, with this review we hope to have begun a discussion in which the fundamental concepts of transport can be brought to bear on the microscopic details of their molecular mechanisms, and *vice versa*.

Acknowledgements

L.R.F. thanks José Faraldo-Gómez and Sebastian Radestock for helpful discussions and Gary Rudnick for useful comments on the manuscript.

References

[1] W.F. Widdas, Inability of diffusion to account for placental glucose transfer in the sheep and consideration of the kinetics of a possible carrier transfer, J. Physiol. 118 (1952) 23–39.
[2] P. Mitchell, A general theory of membrane transport from studies of bacteria, Nature 180 (1957) 134–136.
[3] O. Jardetzky, Simple allosteric model for membrane pumps, Nature 211 (1966) 969–970.
[4] G.A. Vidaver, Inhibition of parallel flux and augmentation of counter flux shown by transport models not involving a mobile carrier, J. Theor. Biol. 10 (1966) 301–306.
[5] C.S. Patlak, Contributions to the theory of active transport: II. The gate type non-carrier mechanism and generalizations concerning tracer flow, efficiency, and measurement of energy expenditure, Bull. Math. Biophys. 19 (1957) 209–235.
[6] W.D. Stein, B. Honig, Models for the active transport of cations...the steady-state analysis, Mol. Cell. Biochem. 15 (1977) 27–44.
[7] M. Klingenberg, in: A.N. Martonosi (Ed.), The enzymes of biological membranes: membrane transport, vol. 3, Plenum Publ. Corp., New York, 1976, pp. 383–438.
[8] W.D. Stein, Transport and diffusion across cell membranes, Academic Press, Orlando, Fl, 1986.
[9] R.M. Krupka, Role of substrate binding forces in exchange-only transport systems: II. Implications for the mechanism of the anion exchanger of red cells, J. Membr. Biol. 109 (1989) 159–171.
[10] I.C. West, Ligand conduction and the gated-pore mechanism of transmembrane transport, Biochim. Biophys. Acta 1331 (1997) 213–234.
[11] R.M. Krupka, Coupling mechanisms in active transport, Biochim. Biophys. Acta 1183 (1993) 105–113.
[12] A.R. Fersht, Enzyme structure and mechanism, Freeman, San Francisco, 1977.
[13] W.P. Jencks, The utilization of binding energy in coupled vectorial processes, Adv. Enzymol. Relat. Areas Mol. Biol. 51 (1980) 75–106.
[14] M. Klingenberg, Ligand-protein interaction in biomembrane carriers. The induced transition fit of transport catalysis, Biochemistry 44 (2005) 8563–8570.
[15] M. Klingenberg, Transport catalysis, Biochim. Biophys. Acta 1757 (2006) 1229–1236.
[16] W.P. Jencks, Utilization of binding energy and coupling rules for active transport and other coupled vectorial processes, Methods Enzymol. 171 (1989) 145–164.
[17] C.J. Law, P.C. Maloney, D.N. Wang, Ins and outs of major facilitator superfamily antiporters, Annu. Rev. Microbiol. 62 (2008) 289–305.
[18] H. Krishnamurthy, C.L. Piscitelli, E. Gouaux, Unlocking the molecular secrets of sodium-coupled transporters, Nature 459 (2009) 347–355.
[19] L.R. Forrest, G. Rudnick, The rocking bundle: a mechanism for ion-coupled solute flux by symmetrical transporters, Physiology 24 (2009) 377–386.
[20] J. Abramson, E.M. Wright, Structure and function of Na^+-symporters with inverted repeats, Curr. Opin. Struct. Biol. 19 (2009) 425–432.
[21] T. Shimamura, S. Weyand, O. Beckstein, N.G. Rutherford, J.M. Hadden, D. Sharples, M.S.P. Sansom, S. Iwata, P.J.F. Henderson, A.D. Cameron, Molecular basis of alternating access membrane transport by the sodium-hydantoin transporter Mhp1, Science 328 (2010) 470–473.

[22] O. Boudker, G. Verdon, Structural perspectives on secondary active transporters, Trends Pharm. Sci. 31 (2010) 418–426.
[23] C. Tanford, Mechanism of free energy coupling in active transport, Annu. Rev. Biochem. 52 (1983) 379–409.
[24] M. Klingenberg, The ADP, ATP shuttle of the mitochondrion, Trends Biochem. Sci. 4 (1979) 249–252.
[25] B. Hille, Ion channels of excitable membranes, 3rd. ed, Sinauer Ass, 2001.
[26] R.M. Krupka, Expression of substrate specificity in facilitated transport systems, J. Membr. Biol. 117 (1990) 69–78.
[27] E. Gouaux, The molecular logic of sodium-coupled neurotransmitter transporters, Philos. T R Soc. B 364 (2009) 149–154.
[28] L. Guan, H.R. Kaback, Lessons from lactose permease, Annu. Rev. Bioph. Biom. 35 (2006) 67–91.
[29] M. Sobczak, J.S. Lolkema, Structural and mechanistic diversity of secondary transporters, Curr. Opin. Microbiol. 8 (2005) 161–167.
[30] E. Padan, L. Kozachkov, K. Herz, A. Rimon, NhaA crystal structure: functional-structural insights, J. Exp. Biol. 212 (2009) 1593–1603.
[31] H. Nury, C. Dahout-Gonzalez, V. Trezeguet, G.J.M. Lauquin, G. Brandolin, E. Pebay-Peyroula, Relations between structure and function of the mitochondrial ADP/ATP carrier, Annu. Rev. Biochem. 75 (2006) 713–741.
[32] E. Pebay-Peyroula, G. Brandolin, Nucleotide exchange in mitochondria: insight at a molecular level, Curr. Opin. Struct. Biol. 14 (2004) 420–425.
[33] M.J. Lemieux, Y.F. Huang, D.N. Wang, The structural basis of substrate translocation by the Escherichia coli glycerol-3-phosphate transporter: a member of the major facilitator superfamily, Curr. Opin. Struct. Biol. 14 (2004) 405–412.
[34] J. Abramson, S. Iwata, H.R. Kaback, Lactose permease as a paradigm for membrane transport proteins, Mol. Membr. Biol. 21 (2004) 227–236.
[35] W. Busch, M.H. Saier, The transporter classification (TC) system, Crit. Rev. Biochem. Mol. 37 (2002) 287–337.
[36] E. Pebay-Peyroula, C. Dahout-Gonzalez, R. Kahn, V. Trezeguet, G.J.M. Lauquin, R. Brandolin, Structure of mitochondrial ADP/ATP carrier in complex with carboxyatractyloside, Nature 426 (2003) 39–44.
[37] E.R. Kunji, P.G. Crichton, Mitochondrial carriers function as monomers, Biochim. Biophys. Acta BBA Bioenerg. 1797 (2010) 817–831.
[38] M. Klingenberg, Wanderings in bioenergetics and biomembranes, Biochim. Biophys. Acta BBA Bioenerg. 1797 (2010) 579–594.
[39] H. Nury, C. Dahout-Gonzalez, V. Trezeguet, G. Lauquin, G. Brandolin, E. Pebay-Peyroula, Structural basis for lipid-mediated interactions between mitochondrial ADP/ATP carrier monomers, FEBS Lett. 579 (2005) 6031–6036.
[40] D.R. Nelson, C.M. Felix, J.M. Swanson, Highly conserved charge-pair networks in the mitochondrial carrier family, J. Mol. Biol. 277 (1998) 285–308.
[41] A.J. Robinson, C. Overy, E.R.S. Kunji, The mechanism of transport by mitochondrial carriers based on analysis of symmetry, Proc. Natl Acad. Sci. USA 105 (2008) 17766–17771.
[42] E.R.S. Kunji, A.J. Robinson, The conserved substrate binding site of mitochondrial carriers, Biochim. Biophys. Acta BBA Bioenerg. 1757 (2006) 1237–1248.
[43] Y. Wang, E. Tajkhorshid, Electrostatic funneling of substrate in mitochondrial inner membrane carriers, Proc. Natl Acad. Sci. USA 105 (2008) 9598–9603.
[44] A.J. Robinson, E.R.S. Kunji, Mitochondrial carriers in the cytoplasmic state have a common substrate binding site, Proc. Natl Acad. Sci. USA 103 (2006) 2617–2622.
[45] W.W. Cleland, Kinetics of enzyme-catalyzed reactions with 2 or more substrates or products, Biochim. Biophys. Acta BBA Bioenerg. 67 (1963) 104–137.
[46] F. Palmieri, Mitochondrial carrier proteins, FEBS Lett. 346 (1994) 48–54.
[47] F. Dehez, E. Pebay-Peyroula, C. Chipot, Binding of ADP in the mitochondrial ADP/ATP carrier is driven by an electrostatic funnel, J. Am. Chem. Soc. 130 (2008) 12725–12733.
[48] S.S. Pao, I.T. Paulsen, M.H. Saier Jr., Major Facilitator Superfamily, Microbiol. Mol. Biol. Rev. 62 (1998) 1–34.
[49] Y. Huang, M.J. Lemieux, J. Song, M. Auer, D.-N. Wang, Structure and mechanism of the glycerol-3-phosphate transporter from *Escherichia coli*, Science 301 (2003) 616–620.
[50] Y. Yin, X. He, P. Szewczyk, T. Nguyen, G. Chang, Structure of the multidrug transporter EmrD from *Escherichia coli*, Science 312 (2006) 741–744.
[51] J. Abramson, I. Smirnova, V. Kasho, G. Verner, H.R. Kaback, S. Iwata, Structure and mechanism of the lactose permease of *Escherichia coli*, Science 301 (2003) 610–615.
[52] L. Guan, O. Mirza, G. Verner, S. Iwata, H.R. Kaback, Structural determination of wild-type lactose permease, Proc. Natl. Acad. Sci. USA 104 (2007) 15294–15298.
[53] O. Mirza, L. Guan, G. Verner, S. Iwata, H.R. Kaback, Structural evidence for induced fit and a mechanism for sugar/H^+ symport in LacY, EMBO J. 25 (2006) 1177–1183.
[54] S. Dang, L. Sun, Y. Huang, F. Lu, Y. Liu, H. Gong, J. Wang, N. Yan, Structure of a fucose transporter in an outward-open conformation, Nature 467 (2010) 734–738.
[55] W. Nie, F.E. Sabetfard, H.R. Kaback, The Cys154 ->Gly mutation in LacY causes constitutive opening of the hydrophilic periplasmic pathway, J. Mol. Biol. 379 (2008) 695–703.
[56] I.N. Smirnova, H.R. Kaback, A mutation in the lactose permease of *Escherichia coli* that decreases conformational flexibility and increases protein stability, Biochemistry 42 (2003) 3025–3031.
[57] Y. Yin, M.Ø. Jensen, E. Tajkhorshid, K. Schulten, Sugar binding and protein conformational changes in lactose permease, Biophys. J. 91 (2006) 3972–3985.
[58] J.B. Klauda, B.R. Brooks, Sugar binding in lactose permease: anomeric state of a disaccharide influences binding structure, J. Mol. Biol. 367 (2007) 1523–1534.
[59] J. Holyoake, M.S.P. Sansom, Conformational change in an MFS protein: MD simulations of LacY, Structure 15 (2007) 873–884.
[60] T. Hirai, S. Subramaniam, Structure and transport mechanism of the bacterial oxalate transporter OxlT, Biophys. J. 87 (2004) 3600–3607.
[61] Y.L. Nie, H.R. Kaback, Sugar binding induces the same global conformational change in purified LacY as in the native bacterial membrane, Proc. Natl Acad. Sci. USA 107 (2010) 9903–9908.
[62] Y.G. Zhou, Y.L. Nie, H.R. Kaback, Residues gating the periplasmic pathway of LacY, J. Mol. Biol. 394 (2009) 219–225.
[63] Y. Nie, Y.G. Zhou, H.R. Kaback, Clogging the periplasmic pathway in LacY, Biochemistry 48 (2009) 738–743.
[64] Z.Y. Liu, M.G. Madej, H.R. Kaback, Helix dynamics in LacY: helices II and IV, J. Mol. Biol. 396 (2010) 617–626.
[65] Y. Nie, N. Ermolova, H.R. Kaback, Site-directed alkylation of LacY: effect of the proton electrochemical gradient, J. Mol. Biol. 374 (2007) 356–364.
[66] H.R. Kaback, R. Dunten, S. Frillingos, P. Venkatesan, I. Kwaw, W. Zhang, N. Ermolova, Site-directed alkylation and the alternating access model for LacY, Proc. Natl Acad. Sci. USA 104 (2007) 491–494.
[67] D.S. Majumdar, I. Smirnova, V. Kasho, E. Nir, X.X. Kong, S. Weiss, H.R. Kaback, Single-molecule FRET reveals sugar-induced conformational dynamics in LacY, Proc. Natl Acad. Sci. USA 104 (2007) 12640–12645.
[68] I.N. Smirnova, V.N. Kasho, H.R. Kaback, Direct sugar binding to LacY measured by resonance energy transfer, Biochemistry 45 (2006) 15279–15287.
[69] I. Smirnova, V. Kasho, J.Y. Choe, C. Altenbach, W.L. Hubbell, H.R. Kaback, Sugar binding induces an outward facing conformation of LacY, Proc. Natl Acad. Sci. USA 104 (2007) 16504–16509.
[70] I. Smirnova, V. Kasho, J. Sugihara, H.R. Kaback, Probing of the rates of alternating access in LacY with Trp fluorescence, Proc. Natl Acad. Sci. USA 106 (2009) 21561–21566.
[71] I. Smirnova, V. Kasho, J. Sugihara, J.Y. Choe, H.R. Kaback, Residues in the H^+ translocation site define the pKa for sugar binding to LacY, Biochemistry 48 (2009) 8852–8860.
[72] I.N. Smirnova, V. Kasho, H.R. Kaback, Protonation and sugar binding to LacY, Proc. Natl Acad. Sci. USA 105 (2008) 8896–8901.
[73] Y. Zhou, L. Guan, J.A. Freites, H.R. Kaback, Opening and closing of the periplasmic gate in lactose permease, Proc. Natl Acad. Sci. USA 105 (2008) 3774–3778.
[74] G. Enkavi, E. Tajkhorshid, Simulation of spontaneous substrate binding revealing the binding pathway and mechanism and initial conformational response of GlpT, Biochemistry 49 (2010) 1105–1114.
[75] D. Yernool, O. Boudker, Y. Jin, E. Gouaux, Structure of a glutamate transporter homologue from *Pyrococcus horikoshii*, Nature 431 (2004) 811–818.
[76] O. Boudker, R.M. Ryan, D. Yernool, K. Shimamoto, E. Gouaux, Coupling substrate and ion binding to extracellular gate of a sodium-dependent aspartate transporter, Nature 445 (2007) 387–393.
[77] N. Reyes, C. Ginter, O. Boudker, Transport mechanism of a bacterial homologue of glutamate transporters, Nature 462 (2009) 880–885.
[78] T. Crisman, S. Qu, B.I. Kanner, L.R. Forrest, Inward-facing conformation of glutamate transporters as revealed by their inverted-topology structural repeats, Proc. Natl Acad. Sci. USA 106 (2009) 20752–20757.
[79] I.H. Shrivastava, J. Jiang, S.G. Amara, I. Bahar, Time-resolved mechanism of extracellular gate opening and substrate binding in a glutamate transporter, J. Biol. Chem. 283 (2008) 28680–28690.
[80] Z. Huang, E. Tajkhorshid, Dynamics of the extracellular gate and ion–substrate coupling in the glutamate transporter, Biophys. J. 95 (2008) 2292–2300.
[81] H.P. Larsson, A.V. Tzingounis, H.P. Koch, M.P. Kavanaugh, Fluorometric measurements of conformational changes in glutamate transporters, Proc. Natl Acad. Sci. USA 101 (2004) 3951–3956.
[82] A. Yamashita, S.K. Singh, T. Kawate, Y. Jin, E. Gouaux, Crystal structure of a bacterial homologue of Na+/Cl− dependent neurotransmitter transporters, Nature 437 (2005) 215–223.
[83] S. Faham, A. Watanabe, G.M. Besserer, D. Cascio, A. Specht, B.A. Hirayama, E.M. Wright, J. Abramson, The crystal structure of a sodium galactose transporter reveals mechanistic insights into Na^+/sugar symport, Science 321 (2008) 810–814.
[84] S. Weyand, T. Shimamura, S. Yajima, S.I. Suzuki, O. Mirza, K. Krusong, E.P. Carpenter, N.G. Rutherford, J.M. Hadden, J. O'Reilly, P. Ma, M. Saidijam, S.G. Patching, R.J. Hope, H.T. Norbertczak, P.C.J. Roach, S. Iwata, P.J.F. Henderson, A.D. Cameron, Structure and molecular mechanism of a nucleobase-cation-symport-1 family transporter, Science 322 (2008) 709–713.
[85] S. Ressl, A.C. Terwisscha van Scheltinga, C. Vonrhein, V. Ott, C. Ziegler, Molecular basis of transport and regulation in the Na^+/betaine symporter BetP, Nature 458 (2009) 47–52.
[86] L. Tang, L. Bai, W.-H. Wang, T. Jiang, Crystal structure of the carnitine transporter and insights into the antiport mechanism, Nat. Struct. Mol. Biol. 17 (2010) 492–496.
[87] S. Schulze, S. Koester, U. Geldmacher, A.C. Terwisscha van Scheltinga, W. Kuehlbrandt, Structural basis of cooperative substrate binding and Na^+-independent transport in the carnitine/butyrobetaine antiporter CaiT, Nature 467 (2010) 233–237.
[88] P.L. Shaffer, A. Goehring, A. Shankaranarayanan, E. Gouaux, Structure and mechanism of a Na^+-independent amino acid transporter, Science 325 (2009) 1010–1014.
[89] Y. Fang, H. Jayaram, T. Shane, L. Kolmakova-Partensky, F. Wu, C. Williams, Y. Xiong, C. Miller, Structure of a prokaryotic virtual proton pump at 3.2 Å resolution, Nature 460 (2009) 1040–1043.
[90] X. Gao, L. Zhou, X. Jiao, F. Lu, C. Yan, X. Zeng, J. Wang, Y. Shi, Mechanism of substrate recognition and transport by an amino acid antiporter, Nature 463 (2010) 828–832.

[91] E. Screpanti, C. Hunte, Discontinuous membrane helices in transport proteins and their correlation with function, J. Struct. Biol. 159 (2007) 261–267.
[92] X. Gao, F. Lu, L. Zhou, S. Dang, L. Sun, X. Li, J. Wang, Y. Shi, Structure and mechanism of an amino acid antiporter, Science 324 (2009) 1565–1568.
[93] S.K. Singh, C.L. Piscitelli, A. Yamashita, E. Gouaux, A competitive inhibitor traps LeuT in an open-to-out conformation, Science 322 (2008) 1655–1661.
[94] S.K. Singh, A. Yamashita, E. Gouaux, Antidepressant binding site in a bacterial homologue of neurotransmitter transporters, Nature 448 (2007) 952–956.
[95] M. Quick, A.-M. Lund Winther, L. Shi, P. Nissen, H. Weinstein, J.A. Javitch, Binding of an octylglucoside detergent molecule in the second substrate (S2) site of LeuT establishes an inhibitor-bound conformation, Proc. Natl Acad. Sci. USA 106 (2009) 5563–5568.
[96] Z. Zhou, J. Zhen, N.K. Karpowich, R.M. Goetz, C.J. Law, M.E.A. Reith, D.-N. Wang, LeuT-desipramine structure reveals how antidepressants block neurotransmitter reuptake, Science 317 (2007) 1390–1393.
[97] Z. Zhou, J. Zhen, N.K. Karpowich, C.J. Law, M.E.A. Reith, D.N. Wang, Antidepressant specificity of serotonin transporter suggested by three LeuT-SSRI structures, Nat. Struct. Mol. Biol. 16 (2009) 652–U696.
[98] L. Shi, M. Quick, Y. Zhao, H. Weinstein, J.A. Javitch, The mechanism of a neurotransmitter:sodium symporter–Inward release of Na + and substrate is triggered by substrate in a second binding site, Mol. Cell 30 (2008) 667–677.
[99] Y. Zhao, D. Terry, L. Shi, H. Weinstein, S.C. Blanchard, J.A. Javitch, Single-molecule dynamics of gating in a neurotransmitter transporter homologue, Nature 465 (2010) 188–193.
[100] L.R. Forrest, Y.-W. Zhang, M.T. Jacobs, J. Gesmonde, L. Xie, B. Honig, G. Rudnick, A mechanism for alternating access in neurotransmitter transporters, Proc. Natl Acad. Sci. USA 105 (2008) 10338–10343.
[101] E. Padan, The enlightening encounter between structure and function in the NhaA Na^+-H^+ antiporter, Trends Biochem. Sci. 33 (2008) 435–443.
[102] C. Hunte, E. Screpanti, M. Venturi, A. Rimon, E. Padan, H. Michel, Structure of a Na^+/H^+ antiporter and insights into mechanism of action and regulation by pH, Nature 435 (2005) 1197–1202.
[103] I.T. Arkin, H. Xu, M.O. Jensen, E. Arbely, E.R. Bennett, K.J. Bowers, E. Chow, R.O. Dror, M.P. Eastwood, R. Flitman-Tene, B.A. Gregersen, J.L. Klepeis, I. Kolossvary, Y. Shan, D.E. Shaw, Mechanism of Na^+/H^+ antiporting, Science 317 (2007) 799–803.
[104] E. Olkhova, E. Padan, H. Michel, The influence of protonation states on the dynamics of the NhaA antiporter from *Escherichia coli*, Biophys. J. 92 (2007) 3784–3791.
[105] Y.-J. Chen, O. Pornillos, S. Lieu, C. Ma, A.P. Chen, G. Chang, X-ray structure of EmrE supports dual topology model, Proc. Natl Acad. Sci. USA 104 (2007) 18999–19004.
[106] S. Schuldiner, EmrE, a model for studying evolution and mechanism of ion-coupled transporters, Biochim. Biophys. Acta BBA Bioenerg. 1794 (2009) 748–762.
[107] S. Schuldiner, When biochemistry meets structural biology: the cautionary tale of EmrE, Trends Biochem. Sci. 32 (2007) 252–258.
[108] I. Ubarretxena-Belandia, J.M. Baldwin, S. Schuldiner, C.G. Tate, Three-dimensional structure of the bacterial multidrug transporter EmrE shows it is an asymmetric homodimer, EMBO J. 22 (2003) 6175–6181.
[109] S.J. Fleishman, S.E. Harrington, A. Enosh, D. Halperin, C.G. Tate, N. Ben-Tal, Quasi-symmetry in the Cryo-EM structure of EmrE provides the key to modeling its transmembrane domain, J. Mol. Biol. 364 (2006) 54–67.
[110] S. Steiner-Mordoch, M. Soskine, D. Solomon, D. Rotem, A. Gold, M. Yechieli, Y. Adam, S. Schuldiner, Parallel topology of genetically fused EmrE homodimers, EMBO J. 27 (2008) 17–26.
[111] V. Agarwal, U. Fink, S. Schuldiner, B. Reif, MAS solid-state NMR studies on the multidrug transporter EmrE, Biochim. Biophys. Acta BBA Bioenerg. 1768 (2007) 3036–3043.
[112] I. Nasie, S. Steiner-Mordoch, A. Gold, S. Schuldiner, Topologically random insertion of EmrE supports a pathway for evolution of inverted repeats in ion-coupled transporters, J. Biol. Chem. 285 (2010) 15234–15244.
[113] T. Eicher, L. Brandstatter, K.M. Pos, Structural and functional aspects of the multidrug efflux pump AcrB, Biol. Chem. 390 (2009) 693–699.
[114] K.M. Pos, Drug transport mechanism of the AcrB efflux pump, Biochim. Biophys. Acta BBA Bioenerg. 1794 (2009) 782–793.
[115] S. Murakami, Multidrug efflux transporter, AcrB–the pumping mechanism, Curr. Opin. Struct. Biol. 18 (2008) 459–465.
[116] M.A. Seeger, A. Schiefner, T. Eicher, F. Verrey, K. Diederichs, K.M. Pos, Structural asymmetry of AcrB trimer suggests a peristaltic pump mechanism, Science 313 (2006) 1295–1298.
[117] S. Murakami, R. Nakashima, E. Yamashita, T. Matsumoto, A. Yamaguchi, Crystal structures of a multidrug transporter reveal a functionally rotating mechanism, Nature 443 (2006) 173–179.
[118] A. Accardi, C. Miller, Secondary active transport mediated by a prokaryotic homologue of ClC Cl^- channels, Nature 427 (2004) 803–807.
[119] C. Miller, ClC chloride channels viewed through a transporter lens, Nature 440 (2006) 484–489.
[120] R. Dutzler, E.B. Campbell, M. Cadene, B.T. Chait, R. MacKinnon, X-ray structure of a ClC chloride channel at 3.0 Å reveals the molecular basis of anion selectivity, Nature 415 (2002) 287–294.
[121] C. Miller, W. Nguitragool, A provisional transport mechanism for a chloride channel-type Cl^-/H^+ exchanger, Philos. T R Soc. B 364 (2009) 175–180.
[122] H. Jayaram, A. Accardi, F. Wu, C. Williams, C. Miller, Ion permeation through a Cl–selective channel designed from a ClC Cl^-/H+ exchanger, Proc. Natl Acad. Sci. USA 105 (2008) 11194–11199.
[123] R. Kramer, M. Klingenberg, Electrophoretic control of reconstituted adenine nucleotide translocation, Biochemistry 21 (1982) 1082–1089.
[124] B. Poolman, Precursor/product antiport in bacteria, Mol. Microbiol. 4 (1990) 1629–1636.
[125] G.F. LeFevre, G.F. McGinnis, Tracer exchange vs. net uptake of glucose through human red cell surface. New evidence for carrier-mediated diffusion, J. Gen. Physiol. (1960) 87–103.
[126] E.M. Wright, The intestinal Na^+/glucose cotransporter, Annu. Rev. Physiol. 55 (1993) 575–589.
[127] L. Parent, S. Supplisson, D.D. Loo, E.M. Wright, Electrogenic properties of the cloned Na^+/glucose cotransporter: I. Voltage-clamp studies, J. Membr. Biol. 125 (1992) 49–62.
[128] M. Sahin-Tóth, A. Karlin, H.R. Kaback, Unraveling the mechanism of the lactose permease of *Escherichia coli*, Proc. Natl Acad. Sci. USA 97 (2000) 10729–10732.
[129] H.R. Kaback, M. Sahin-Toth, A.B. Weinglass, The kamikaze approach to membrane transport, Nat. Rev. Mol. Cell Biol. 2 (2001) 610–620.
[130] S.C. King, T.H. Wilson, Towards an understanding of the structural basis of 'forbidden' transport pathways in the *Escherichia coli* lactose carrier: mutations probing the energy barriers to uncoupled transport, Mol. Microbiol. 4 (1990) 1433–1438.
[131] R.J. Brooker, An analysis of lactose permease "sugar specificity" mutations which also affect the coupling between proton and lactose transport. I. Val177 and Val177/Asn319 permeases facilitate proton uniport and sugar uniport, J. Biol. Chem. 266 (1991) 4131–4138.
[132] J.S. Lolkema, B. Poolman, Uncoupling in secondary transport proteins. A mechanistic explanation for mutants of lac permease with an uncoupled phenotype, J. Biol. Chem. 270 (1995) 12670–12676.
[133] J.L. Johnson, R.J. Brooker, Control of H^+/lactose coupling by ionic interactions in the lactose permease of *Escherichia coli*, J. Membr. Biol. 198 (2004) 135–146.
[134] G.J. Kaczorowski, H.R. Kaback, Mechanism of lactose translocation in membrane vesicles from *Escherichia coli*. 1. Effect of pH on efflux, exchange, and counterflow, Biochemistry 18 (1979) 3691–3697.
[135] G.J. Kaczorowski, D.E. Robertson, H.R. Kaback, Mechanism of lactose translocation in membrane vesicles from *Escherichia coli*. 2. Effect of imposed delata psi, delta pH, and Delta mu H^+, Biochemistry 18 (1979) 3697–3704.
[136] D.E. Robertson, G.J. Kaczorowski, M.L. Garcia, H.R. Kaback, Active transport in membrane vesicles from *Escherichia coli*: the electrochemical proton gradient alters the distribution of the lac carrier between two different kinetic states, Biochemistry 19 (1980) 5692–5702.
[137] J.J. Garcia-Celma, J. Ploch, I. Smirnova, H.R. Kaback, K. Fendler, Delineating electrogenic reactions during lactose/H(+) symport, Biochemistry 49 (2010) 6115–6121.
[138] J.J. Garcia-Celma, I.N. Smirnova, H.R. Kaback, K. Fendler, Electrophysiological characterization of LacY, Proc. Natl Acad. Sci. USA 106 (2009) 7373–7378.
[139] M. Klingenberg, Transport viewed as a catalytic process, Biochimie 89 (2007) 1042–1048.
[140] Y. Zhou, E. Zomot, B.I. Kanner, Identification of a lithium interaction site in the γ-aminobutyric acid (GABA) transporter GAT-1, J. Biol. Chem. 281 (2006) 22092–22099.
[141] K.M.Y. Penado, G. Rudnick, M.M. Stephan, Critical amino acid residues in transmembrane span 7 of the serotonin transporter identified by random mutagenesis, J. Biol. Chem. 273 (1998) 28098–28106.
[142] S.A. Mari, A. Soragna, M. Castagna, E. Bossi, A. Peres, V.F. Sacchi, Aspartate 338 contributes to the cationic specificity and to driver-amino acid coupling in the insect cotransporter KAAT1, Cell. Mol. Life Sci. 61 (2004) 243–256.
[143] S. Mager, N. Kleinberger-Doron, G.I. Keshet, N. Davidson, B.I. Kanner, H.A. Lester, Ion binding and permeation at the GABA transporter GAT1, J. Neurosci. 16 (1996) 5405–5414.
[144] S.Y. Noskov, B. Roux, Control of ion selectivity in LeuT: two Na^+ binding sites with two different mechanisms, J. Mol. Biol. 377 (2008) 804–818.
[145] D.A. Caplan, J.O. Subbotina, S.Y. Noskov, Molecular mechanism of ion–ion and ion–substrate coupling in the Na^+-dependent leucine transporter LeuT, Biophys. J. 95 (2008) 4613–4621.
[146] L. Celik, B. Schiott, E. Tajkhorshid, Substrate binding and formation of an occluded state in the leucine transporter, Biophys. J. 94 (2007) 1600–1612.
[147] A. de la Vieja, M.D. Reed, C.S. Ginter, N. Carrasco, Amino acid residues in transmembrane segment IX of the Na^+/I^- symporter play a role in its Na^+ dependence and are critical for transport activity, J. Biol. Chem. 282 (2007) 25290–25298.
[148] Y. Zhou, E.R. Bennett, B.I. Kanner, The aqueous accessibility in the external half of transmembrane domain I of the GABA transporter GAT-1 is modulated by its ligands, J. Biol. Chem. 279 (2004) 13800–13808.
[149] J. Li, E. Tajkhorshid, Ion-releasing state of a secondary membrane transporter, Biophys. J. 97 (2009) L29–L31.
[150] L.R. Forrest, S. Tavoulari, Y.-W. Zhang, G. Rudnick, B. Honig, Identification of a chloride ion binding site in Na+/Cl− dependent transporters, Proc. Natl Acad. Sci. USA 104 (2007) 12761–12766.
[151] E. Zomot, A. Bendahan, M. Quick, Y. Zhao, J.A. Javitch, B.I. Kanner, Mechanism of chloride interaction with neurotransmitter:sodium symporters, Nature 449 (2007) 726–730.
[152] Z. Tao, A. Gameiro, C. Grewer, Thallium ions can replace both sodium and potassium ions in the glutamate transporter Excitatory Amino Acid Carrier 1, Biochemistry 47 (2008) 12923–12930.
[153] S. Teichman, S. Qu, B.I. Kanner, The equivalent of a thallium binding residue from an archeal homolog controls cation interactions in brain glutamate transporters, Proc. Natl Acad. Sci. USA 106 (2009) 14297–14302.
[154] H.P. Larsson, X. Wang, B. Lev, I. Baconguis, D.A. Caplan, N.P. Vyleta, H.P. Koch, A. Diez-Sampedro, S.Y. Noskov, Evidence for a third sodium-binding site in

glutamate transporters suggests an ion–substrate coupling model, Proc. Natl Acad. Sci. USA 107 (2010) 13912–13917.
[155] Z. Tao, N. Rosental, B.I. Kanner, A. Gameiro, J. Mwaura, C. Grewer, Mechanism of cation binding to the glutamate transporter EAAC1 probed with mutation of the conserved amino acid residue T101, J. Biol. Chem. 285 (2010) 17725–17733.
[156] D.C. Holley, M.P. Kavanaugh, Interactions of alkali cations with glutamate transporters, Philos. T R Soc. B 364 (2009) 155–161.
[157] Z. Huang, E. Tajkhorshid, Identification of the third Na^+ site and the sequence of extracellular binding events in the glutamate transporter, Biophys. J. 99 (2010) 1416–1425.
[158] D. Menaker, A. Bendahan, B.I. Kanner, The substrate specificity of a neuronal glutamate transporter is determined by the nature of the coupling ion, J. Neurochem. 99 (2006) 20–28.
[159] J.I. Wadiche, M.P. Kavanaugh, Macroscopic and microscopic properties of a cloned glutamate transporter/chloride channel, J. Neurosci. 18 (1998) 7650–7661.
[160] N. Watzke, E. Bamberg, C. Grewer, Early intermediates in the transport cycle of the neuronal excitatory amino acid carrier EAAC1, J. Gen. Physiol. 117 (2001) 547–562.
[161] P.J. Franco, R.J. Brooker, Functional roles of Glu-269 and Glu-325 within the lactose permease of *Escherichia coli*, J. Biol. Chem. 269 (1994) 7379–7386.
[162] M.L. Ujwal, M. Sahin-Toth, B. Persson, H.R. Kaback, Role of glutamate-269 in the lactose permease of *Escherichia coli*, Mol. Membr. Biol. 11 (1994) 9–16.
[163] D. Wang, G.A. Voth, Proton transport pathway in the ClC Cl^-/H^+ antiporter, Biophys. J. 97 (2009) 121–131.
[164] H.-H. Lim, C. Miller, Intracellular proton-transfer mutants in a CLC Cl^-/H^+ exchanger, J. Gen. Physiol. 133 (2009) 131–138.
[165] M.J. Roux, S. Supplisson, Neuronal and glial glycine transporters have different stoichiometries, Neuron 25 (2000) 373–383.
[166] S. Murakami, R. Nakashima, E. Yamashita, A. Yamaguchi, Crystal structure of bacterial multidrug efflux transporter AcrB, Nature 419 (2002) 587–593.